Gorowitz, B., T. B. Gorezyea, and R. J. Saia: *Solid State Technol.*, p. 179, June 1985.
Greene, J. E., and S. A. Barnett: *J. Vac. Sci. Technol.*, vol. 21, p. 285, 1982.
Harper, J. M. F., J. J. Cuomo, P. A. Leary, G. M. Summa, H. R. Kaufmann, and F. J. Bresnock: *J. Electrochem. Soc.*, vol. 128, p. 1077, 1981.
Hasted, J. B.: *Physics of Atomic Collision*, Butterworth, London, 1964.
Hess, D. W.: *Ann. Rev. Mater. Sci.*, vol. 16, p. 163, 1986.
Horwitz, C. M.: *J. Vac. Sci. Technol.*, vol. A1, p. 90, 1983.
Kemper, M. J. H., S. W. Koo, and F. Huizinga: in G. S. Mathad *et al.* (eds.), *Plasma Processing*, The Electrochemical Society, Pennington, N.J., 1985.
Kettani, M. A., and M. F. Hoyaux: *Plasma Engineering*, Wiley, New York, 1973.
Langmuir, I.: *General Electric Rev.*, vol. 26, p. 731, 1923.
——— and H. Mott-Smith: *General Electric Rev.*, vol. 27, pp. 449, 538, 616, 762, 810, 1924.
Ligenza, J. R.: *J. Appl. Phys.*, vol. 36, p. 2703, 1965.
Maissel, L.: in L. Maissel and R. Glang (eds.), *Handbook of Thin Film Technology*, chap. 4, McGraw-Hill, New York, 1970.
Meyerson, B. S., E. Ganin, D. A. Smith, and T. N. Nguyen: *J. Electrochem. Soc.*, vol. 133, p. 1232, 1986.
Mogab, C. J., A. C. Adams, and D. L. Flamm: *J. Appl. Phys.*, vol. 49, p. 3769, 1978.
Morgan, R. A.: *Plasma Etching in Semiconductor Fabrication*, Elsevier, London, 1985.
Nguyen, V. S., J. Underhill, S. Fridmann, and P. Pan: in G. S. Mathad *et al.* (eds.), *Plasma Processing*, The Electrochemical Society, Pennington, N.J., 1985.
Petro, W. G., B. R. Cairns, and K. V. Anand: in H. Huff *et al.* (eds.), *Semiconductor Silicon 1986*. The Electrochemical Society, Pennington, N.J. 1986.
Steinbruchel, C.: *J. Vac. Sci. Technol.*, vol. A3, p. 1913, 1985.
Sugiura, H., and M. Yamaguchi: *Jap. J. Appl. Phys.*, vol. 19, p. 583, 1980.
Tu, Y. Y., T. J. Chuang, and H. F. Winters: IBM Research Report RY 2810, 1981.
Turban, G.: *Pure and Appl. Chem.*, vol. 56, p. 215, 1984.
Vratny, F.: *J. Electrochem. Soc.*, vol. 114, p. 505, 1967.
Wehner, G. K., and G. S. Anderson: in L. Maissel and R. Glang (eds.), *Handbook of Thin Film Technology*, chap. 3, McGraw-Hill, New York, 1970.

CHAPTER 10

PHYSICAL VAPOR DEPOSITION APPARATUSES AND PLASMA REACTORS

10.1 INTRODUCTION

Apparatuses and reactors used for physical and physicochemical processes are diverse. They range from vacuum deposition apparatuses, sputtering equipment, elaborate molecular beam epitaxy (MBE) apparatuses, and various types of plasma reactors. Physical sputtering and MBE are the principal physical vapor deposition (PVD) processes. Physical sputtering remains a major method of metallization in which metals are deposited. MBE is the preferred choice for epitaxial deposition of thin films of III-V compounds, particularly when heterostructures with sharp doping profiles are desired. Any apparatus for PVD requires an elaborate vacuum system.

The phenomena taking place in a plasma reactor are quite complex. The added complications, compared to conventional CVD reactors, arise from the presence of plasma, a medium that literally determines the fate of deposition or etching. At the core of the complications are the collision processes in plasma leading to the formation of electrons, ions, and reactive neutral species, the transport phenomena within the plasma and in the sheaths, and their relation to the

electrical characteristics of the plama. These phenomena interact with transport phenomena in the reactor and heterogeneous reactions on substrate surfaces.

For PVD, attention will be focused on apparatus used for sputtering and MBE in this chapter. Then diffusion of charged particles in plasma reactors will be considered. This will be followed by a section on the characteristics of plasma and their relation to measurable electrical variables. These can be combined with intrinsic kinetics and reactor conservation equations to describe plasma reactors, leading to design considerations for plasma reactors. Because of the complexities, many of the relationships for plasma are approximate, in particular those related to plasma characteristics. Further, only a few principal species, mainly responsible for plasma deposition or etching, can be considered. In spite of the complexities and approximations, certain limits and trends can be ascertained from the approximate relationships and the main species of interest.

10.2 PHYSICAL VAPOR DEPOSITION (PVD) APPARATUSES

An apparatus for vacuum deposition is shown in Fig. 10-1. As discussed in Chap. 9, a planetary surface receives the same amount of mass flux from a source. The arrangement of substrates in the figure takes advantage of this fact. The rest of the apparatus is for maintaining the desired vacuum level in the deposition chamber.

In contrast to the apparatus used for vacuum metal deposition (usually amorphous), the apparatus for MBE is much more complex and elaborate because of the epitaxy requirements. A schematic of a vacuum chamber in which MBE is carried out is shown in Fig. 10-2. Today the trend is toward the use of effusion cells to which liquid gas source species are introduced. Originally, melts were used exclusively for evaporant sources, and an electron gun was used to

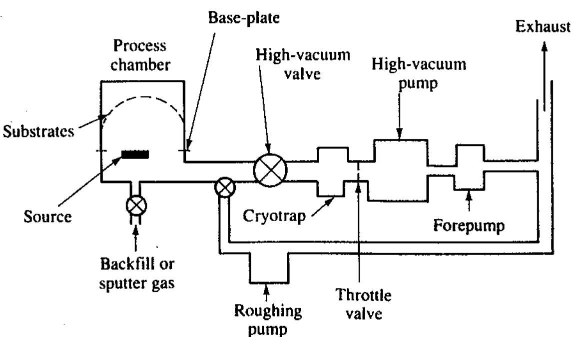

FIGURE 10-1
Schematic of a system for vacuum deposition (Fraser, 1983).

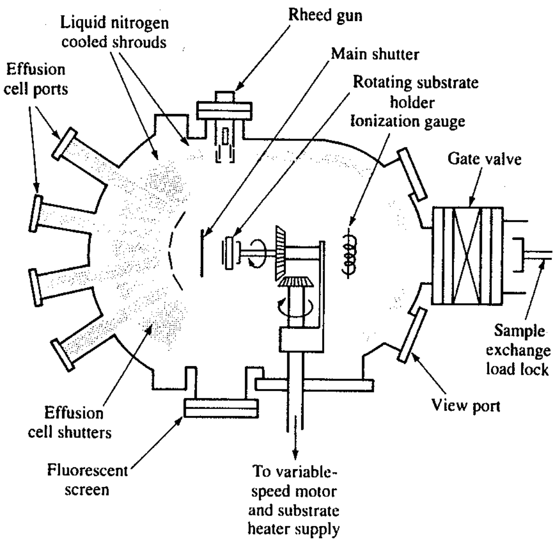

FIGURE 10-2
An MBE apparatus (Cho, 1987).

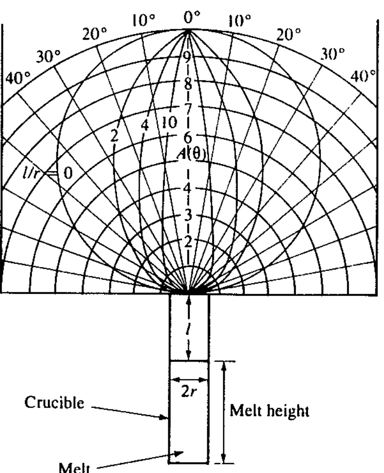

FIGURE 10-3
Angular distribution of flux from a crucible (Luscher and Collins, 1981).

produce source materials of high boiling point, such as silicon (see Fig. 10-2). There are several reasons for the change. As discussed in Chap. 9, MBE is most suitable for thin films with abrupt and well-defined doping profiles which can be realized at lower temperatures. Therefore, the use of MBE has been shifting to the preparation of such thin films for III-V compound semiconductors, typically used for optoelectronic applications. The shift has also been prompted by the fact that MBE film qualities are in general poorer than CVD film but the thin films with abrupt doping profiles necessary for optoelectronic devices are easier to obtain by MBE. For III-V compound semiconductors, liquid/gas source species are readily available and they are more convenient to use. Another reason for the change has to do with the ease with which film-thickness uniformity can be achieved with the liquid/gas source in "effusion" cells. With the melt source, the thickness distribution is determined by the cosine law. This is shown in Fig. 10-3, which gives angular distribution of flux by evaporation from a crucible as a function of time. In contrast, the source gas (vaporized, if liquid, by heating) is fed externally to the effusion cell as shown in Fig. 10-2. Because the external gas is fed into vacuum, the gas "jets" and as a result the trajectories of the gas molecules are well defined. This is shown in Fig. 10-4. As the figure illustrates, the trajectories are confined to the length (or diameter) of a substrate if the centerline of the effusion cell passes through the substrate center and if the extensions of the cell walls form straight lines with the substrate edges. Although the flux arriving at the substrate is dependent on the substrate position, uniform deposition is possible with the rotation of the substrate since then all parts of the surface receive equal exposure to the varying flux.

Although MBE used to be strictly by evaporation/condensation, such a distinction is no longer valid, particularly with the gas source material used in effusion cells. With the substrate temperatures higher than 400 °C and pressures in the 10^{-5} torr range, the epitaxial growth for III-V compound films is more likely due to heterogeneous surface reactions than to simple condensation. The similarity is particularly apparent in light of the fact that the substrate temperature in MBE is kept as high as the desired doping profile will allow to

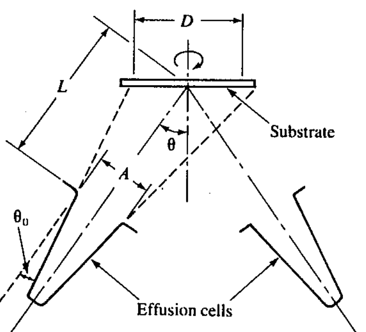

FIGURE 10-4
Trajectories of flux from effusion cells (Saito *et al.*, 1986).

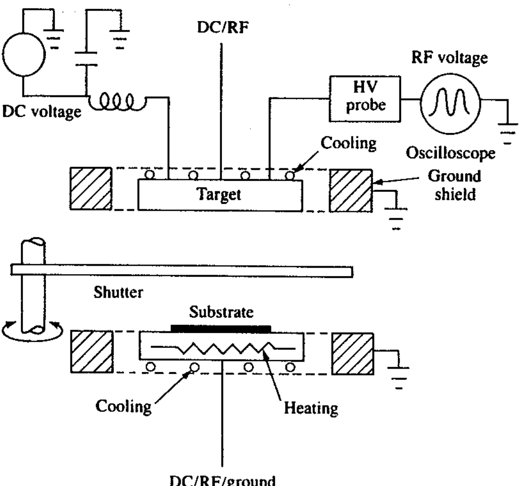

FIGURE 10-5
Schematic of a sputtering system (Chapman, 1980).

achieve better film qualities. In fact, the atomic layer epitaxy (ALE) discussed in Chap. 5 is essentially the same as the MBE with gaseous source species.

A schematic of a sputtering system is shown in Fig. 10-5. As shown in the figure, it can be operated as either a dc or rf discharge. The target is surrounded by a dark space shield, also known as a ground shield. This feature restricts ion bombardment and sputtering only to the target. To prevent ion bombardment of the protected regions, the space between the target and the ground shield must be less than the thickness of the dark space (sheath). Otherwise, a self-sustained discharge can form in the space. As will be shown in subsequent sections, the sheath thickness decreases with increasing pressure. Thus, the size of the gap between the target and shield sets an upper pressure limit for operating the system. The sheath thickness also decreases with increasing frequency in rf sputtering.

Another feature shown in Fig. 10-5 is a shutter that can be rotated into place between the electrodes. The shutter is typically used during a presputtering period when a few atomic layers of the target are sputtered away for removing any impurities that might be present on the target surface. In this way any contaminants introduced during loading, unloading, or *in situ* substrate cleaning can be removed from the target. Sputtering takes place entirely by momentum transfer and as such considerable heating of the target occurs. The localized heating can be excessive (up to 400 °C; Chapman 1980) and can lead to damage of the bonding between the target and the backing electrode or of the target itself. Thus, the target is usually cooled. However, various mechanical problems associated

with cooling can be avoided if the power input is not too high. The desired substrate temperature is usually obtained by resistance heating. Here, again, cooling on the backside is required, as shown in Fig. 10-5.

The effect of current and voltage on the deposition rate by physical sputtering can be inferred directly from Eq. (9.13), which represents the maximum possible rate of deposition:

$$r_s = \frac{SJ_i}{q} \tag{9.13}$$

where S is the sputtering yield (atoms ejected per incident ion), J_i is the ion current density, and q is the electric charge. The effect of the current is larger than that of the voltage since the sputtering yield is proportional to the square root of the voltage [with a bias with respect to the threshold energy; see Eq. (9.11)] but J_i is directly proportional to the current. Therefore, for a given power, it is best to sputter at high current and low voltage for higher deposition rates. This can be achieved by using a thermionically supported glow or by going to higher pressure. As the pressure in a sputtering system is raised, the ion density and therefore the current density increases. The upper limit is set by the requirement of eliminating plasma formation in the space between the target and ground shield. The usual range for physical sputtering is from 20 to 130 mtorr, but the optimal range is 50 to 60 mtorr for dc discharges (Maissel, 1970). The rate of deposition decreases with increasing temperature. This is due to the fact that the deposition is by condensation. The cosine law also applies to deposition.

10.3 PLASMA REACTORS

Reactors for plasma processing were originally developed for etching. Some of these reactors were adapted for plasma deposition. Although the plasma reactors have been in use since the early 1970s, they are still in their infancy in terms of our ability to describe them mathematically. However, systematic studies have already been undertaken, particularly for etching (Alkire and Economou, 1985; Dalvie *et al.*, 1986; Stenger *et al.*, 1987).

Plasma reactors for etching are shown in Fig. 10-6. The so-called barrel reactor in Fig. 10-6*a*, which physically resembles a conventional LPCVD reactor, was the first plasma reactor in semiconductor processing. Initially it was mainly for stripping of photoresist in an oxygen plasma (Irving, 1971) and later for the etching of dielectric materials such as SiO_2, typically in CF_4/O_2 mixtures. As shown in the figure, the reactor consists of a cylindrical quartz chamber that has input gas manifolds and a vacuum pumping outlet to maintain the pressure at around 1 torr. Although the schematic shows the gas being fed from the top, it is also fed from the bottom in other arrangements. The plasma is sustained by an rf potential applied to two external electrodes. Usually, a perforated aluminum cylinder is placed coaxially around the wafers which are stacked on a boat as shown in the figure. In such an arrangement, the plasma is confined in the

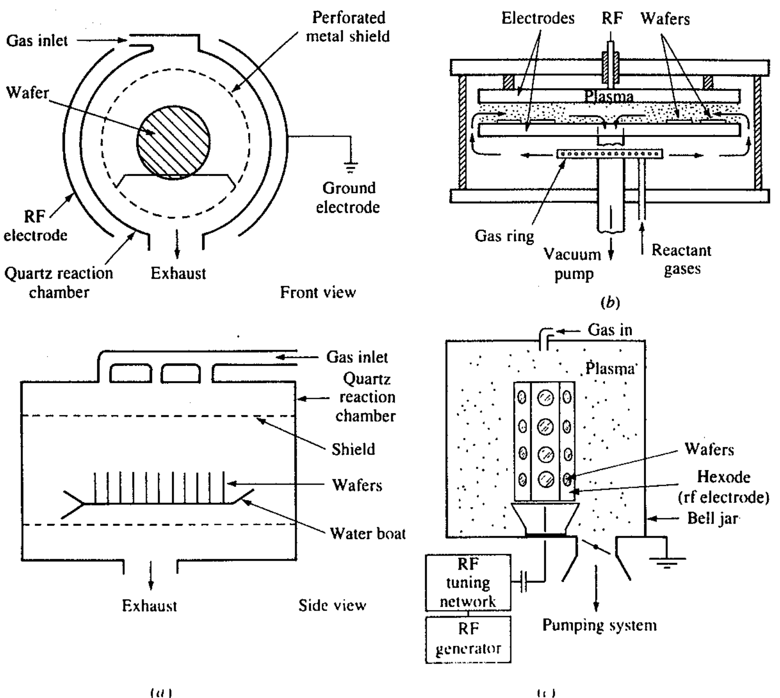

FIGURE 10-6
Plasma reactors for etching: (*a*) barrel reactor, (*b*) planar (radial) reactor (Reinberg, 1975; Heinecke, 1975), and (*c*) hexode (Bell Lab) reactor

annular regions between the metal cylinder and the reactor wall. The mesh of the aluminum tunnel surrounding the wafers is sufficient to allow the passage of active neutral species while limiting the number of ions passing through. The aluminum tunnel is usually mounted in such a way that it electrically floats. With such an arrangement, a minimum of energetic ionized components are allowed to enter the tunnel from the plasma region (Morgan, 1985). This can partially prevent the overheating of the wafer surface by bombarding ions that can lead to poor uniformity of etching and poor selectivity. Before commencement of etching, some wafer temperature control can be attained by preheating the wafers in an inert gas plasma.

It should be evident from the reactor configuration that ion bombardment does not have any significant role in the barrel reactor. As such, the etching selectivity can be very high, as high as 100:1 for the selectivity of Si:SiO_2. The other consequence of such a configuration is that no anisotropy can be achieved.

Therefore, the barrel reactor cannot be used where linewidth control is critical. However, it does give a high throughput for applications not involving close linewidth control. Another aspect particular to the barrel reactor is that the concentration of active neutrals, which are responsible for etching, decreases as they travel from the tunnel mesh to the wafers because of recombination reactions.

Perhaps the most widely used plasma reactor for etching is the planar reactor shown in Fig. 10-6*b*. The reactor arrangement takes full advantage of the effects of ion bombardment. It allows for enhancement of etching due to the surface modification by bombarding ions and for anisotropy. The reactor typically consists of a top electrode that is powered by an rf supply and a bottom electrode that is normally grounded. The wafers are usually placed on the grounded electrode and are in "contact" with the plasma, as opposed to the barrel reactor. Note that a planar reactor will etch wafers located on either electrode surface. The wafer surface is bombarded by ions accelerated by the sheath potential. As shown in Fig. 10-6*b*, the etching gas is fed through a gas ring, which is in turn evacuated by a vacuum pump. In the arrangement shown in the figure, the wafers are immersed in the plasma.

In general, the disadvantages of the barrel reactor are the advantages of planar reactor and vice versa. The anisotropy attainable in a planar reactor is the major feature of the reactor.

One problem in planar reactors has to do with the physical sputtering that takes place on the electrode. The situation is aggravated by having the whole electrode surfaces facing each other. A reactor developed by Bell Laboratories to minimize the physical sputtering of electrodes is called the hexode (Bell Lab) reactor and is shown in Fig. 10-6*c*; it is similar in its physical appearance to the conventional CVD barrel reactor. The hexode on which wafers are placed is connected to an external rf generator as shown in the figure and the reactor wall is grounded. The hexode side walls face in different directions to partially prevent sputtered material from depositing on the wafer surface. In this arrangement, the wafers are on a powered electrode and thus are subject to a larger sheath potential.

Most plasma reactors are preconditioned for etching before wafers are placed to warm the reactor and to reduce wafer contamination. Wafers are introduced to the reactor through a load lock to minimize atmospheric contamination, especially water vapor. Optical emission spectra and mass spectroscopy are used to detect the endpoint of etching. The electrode materials used in reactors are usually anodized aluminum or titanium, which are relatively inert catalytically. Some atoms of electrode material are always present due to physical sputtering, and they in turn can catalyze polymer formation as in CCl_4 plasma (Tokauaga and Hess, 1980).

Reactors for plasma deposition are essentially the same as those for plasma etching. The barrel reactor in Fig. 10-6*a* has been used for plasma deposition and so has the planar reactor. A variation of the planar arrangement, particularly with respect to feeding, is shown in Fig. 10-7*a*. A distinct feature is the presence of a heater, since the deposition is carried out at much higher substrate temperatures than those for etching. A distinct departure from the reactors that were originally used for etching is shown in Fig. 10-7*b* for plasma deposition. The deposition chamber is in the form of a resistance-heated quartz furnace tube. Wafers are loaded onto both faces of an array of parallel graphite electrodes. Alternate electrodes in the array are connected to an external rf source. The reactant gas stream is directed along the axis of the chamber tube and between the electrodes. The plasma is ignited between adjacent electrodes. Another distinct feature is the use of pulsed rf excitation rather than the continuous excitation. Good thickness uniformity over large batch sizes and better temperature control are cited (Kumagai, 1984) for the reactor. More discussions on the reactors for plasma deposition can be found in the article by Weiss (1983).

The design objectives of plasma reactors for etching are high throughput, etching uniformity, high selectivity, and anisotropy (when linewidth control is

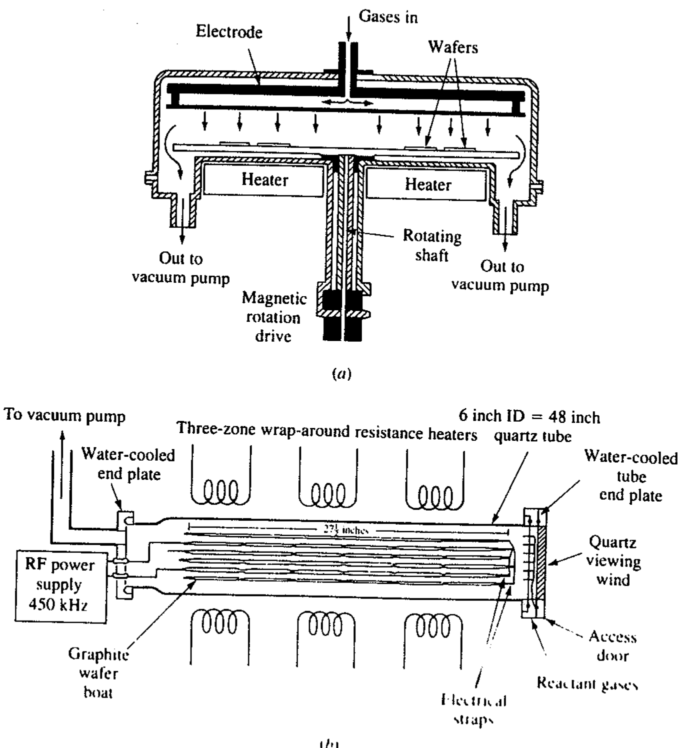

FIGURE 10-7
Plasma reactors for deposition: (*a*) planar reactor with perforated electrode (Applied Materials, Inc.) and (*b*) an LPCVD-type deposition chamber (Kumagai, 1984).

critical). Contamination or side effects due to physical sputtering is another problem that such a reactor has to deal with. The design objectives of plasma reactors for deposition are essentially the same as those for the conventional CVD reactors, namely thickness uniformity and high throughput. As discussed in Chap. 5 for CVD reactors, there are also constraints. These constraints, such as those from film-quality considerations, provide a region of feasibility within which a reactor can be designed and operated.

For plasma reactors, the characteristics pertinent to the plasma have to be considered. They are determined by applied excitation power, excitation frequency, pressure, and a diffusion length characteristic of the reactor dimensions. These plasma characteristics are the same whether deposition or etching is involved. The only distinction is that a different aspect of the plasma characteristics is important for deposition (which involves deposition of reactive neutrals) versus etching (which involves gasification of substrate by reactive neutrals). Although the total pressure is important in CVD reactors, because of its role in determining flow regimes and enhancing diffusion, the pressure effects in plasma reactors should be viewed in terms of collisions. To begin with, a plasma is generated by collisions of electrons with neutral molecules and, as such, the pressure has a dominant effect on plasma characteristics. The typical total pressure in plasma reactors is at most 10 torr. The molecular flow regime is rarely encountered in plasma reactors since the plasma extinguishes when the electron mean free path approaches the magnitude of reactor dimension. It is noted in this regard that the mean free path of electrons is several times that of neutrals. The low limit on the pressure is dictated by the need to sustain a plasma. The limit decreases with increasing power and excitation frequency. The practical range is much higher than the low limit since an efficient discharge requires sufficient collisions. To gain an understanding of plasma characteristics, transport properties of charged particles (electrons and ions) are considered first.

10.4 TRANSPORT PROPERTIES OF IONS AND ELECTRONS

The transport properties of interest in plasma processing are diffusivities and mobilities of electrons and ions in a fluid medium. The mobility is the transport property that relates the external force (electric field) to the flux of charged particles due to the force. This flux is called "drift flux." An analogy in mass transport can be found where convective flux is caused by the external force of pressure. Thus, the drift flux is equivalent to the convective flux. The mobility relates the electric field to drift velocity, v_d, as follows:

$$v_d = \mu E \tag{10.1}$$

where μ is the mobility and E is the electric field. It has the unit of square centimetres per volt-second. Here again, the drift velocity is equivalent to fluid velocity in convective flow.

As in mass transport, the flux of charged particles consists of diffusive flux and drift (convective) flux:

$$j_i = -D_i \frac{dn_i}{dx} + \mu_i E n_i \tag{10.2}$$

$$j_e = -D_e \frac{dn_e}{dx} - \mu_e E n_e \tag{10.3}$$

which are the one-dimensional expressions for the (positive) ion flux j_i and the electron flux j_e. Here D_i and D_e are the diffusivities of ions and electrons, respectively, and μ_i and μ_e are the mobilities of ions and electrons. Note in Eq. (10.3) that the drift term is negative since electrons move in the direction opposite to the electric field.

According to the kinetic theory of Chapman-Enskog, the ion-atom mutual diffusion coefficient D_i is given to second order by

$$D_i = \frac{3\pi^{1/2}}{16}\left(\frac{2k_B T}{M_r}\right)^{7/2} \frac{1 + E_o}{(n_i + n_a)P_{ia}} \tag{10.4}$$

where M_r is the reduced mass given by $M_i M_a/(M_i + M_a)$, n_i is the ion and n_a the atom number densities, E_o is a second-order correction which may be taken as zero, and P_{ia} is an average of diffusion cross section over a Maxwellian velocity distribution. Often, it is of interest to find the dependence of the diffusivity on pressure and temperature. Because of the dependence of P_{ia} on the pressure and temperature, the diffusivity is given by

$$D_i = (\text{constant}) \frac{T^m}{M_r P} \tag{10.5}$$

where P is the total pressure and m can take on a value of 2 for low temperature or 1.66 for high temperature. In plasmas, n_i is much less than n_a and, if one assumes the elastic sphere model (Hirschfelder *et al.*, 1964), Eq. (10.4) reduces to

$$D_i = \frac{3}{8}\left(\frac{\pi k_B T}{2M_r}\right)(n_a \pi d_{ia}^2)^{-1} \qquad \text{where } d_{ia} = \frac{d_i + d_a}{2} \tag{10.6}$$

and d_i and d_a, respectively, are the ion and atom diameters. The mobility can then be obtained from the Einstein relation:

$$\frac{D_i}{\mu_i} = \frac{k_B T_i}{q} \tag{10.7}$$

The temperature and pressure dependence of the mobility can be written (McDaniel, 1964) as

$$\mu_i = (\text{constant}) \frac{T_i^n}{M_r^{1/2} P} \tag{10.8}$$

where n is zero at low temperature and $-\frac{1}{3}$ at high temperature. Here the temperature dependence of mobility is different from that expected from the Einstein relation because of the temperature dependence of velocity.

The Einstein relation, which is applicable to a system at thermal equilibrium, has to be modified for electrons in a fluid:

$$\frac{D_e}{\mu_e} = \frac{\lambda_t k_B T_e}{q} \tag{10.9}$$

where the Townsend coefficient λ_t (McDaniel, 1964) accounts for the nonequilibrium nature of the electrons. The coefficient increases nonlinearly with E/P. Use of Eq. (10.1) for electrons in Eq. (10.9) leads to

$$(v_d)_e = (\text{constant}) \frac{E/P}{\lambda_t T_e} \tag{10.10}$$

Experimental results for the drift velocity are usually correlated to E/P, typically on a log-log scale as shown in Fig. 10-8. For most gases, the drift velocity is of the order of 10^6 cm/s for electrons and of 10^5 cm/s for ions at E/P of 1 volt/(cm·torr). Once the drift velocity of electrons is known, the diffusivity can be calculated from Eq. (10.9).

The diffusivities are often calculated from experimental "ambipolar" diffusivities. When the density of electrons and ions becomes large (usually larger than

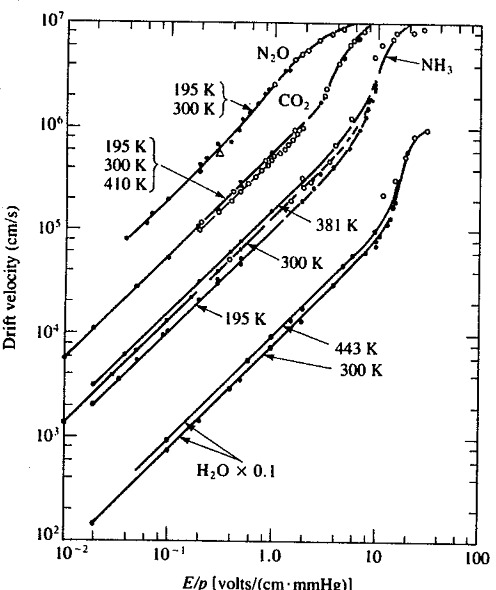

FIGURE 10-8
Drift velocity for several gases (McDaniel, 1964).

10^8 cm^{-3}), the ordinary diffusion does not hold because of their mutual Coulomb fields. The diffusivity of electrons is about four orders of magnitude higher than that of ions, a typical electron diffusivity being 10^6 cm^2/s. Thus, electrons attempt to diffuse more rapidly than ions toward regions of lower concentration, but their motion is impeded by the restraining space charge field thereby created. This same field has the opposite effect on the ions and causes them to diffuse at a faster rate than they would in the absence of the electrons. Both species of charged particles consequently diffuse with the same velocity, and since there is now no difference in the flow of the particles of opposite sign the diffusion is called ambipolar (McDaniel, 1964). Consider a fluid medium in which the density of electrons is the same as that of ions. Let this density be n and the velocity be v_a, which is the same for both species. Use of these in Eqs. (10.2) and (10.3), where now $j = j_i = j_e = v_a n$ and $n = n_i = n_e$, leads to the following definition of the (see Prob. 10.2) ambipolar diffusivity D_a:

$$D_a = \frac{D_e \mu_i + D_i \mu_e}{\mu_i + \mu_e} \tag{10.11}$$

Approximate relationships result from Eq. (10.11) and the Einstein relation (with Townsend coefficient of unity) when $\mu_i \gg \mu_e$ and $T_e \gg T_i$:

$$D_a = \begin{cases} \dfrac{k_B T_e}{q} \mu_i & (10.12) \\ D_i\left(1 + \dfrac{T_e}{T_i}\right) = D_i \dfrac{T_e}{T_i} & (10.13) \end{cases}$$

Note that $D_a P$ is a constant, and experimental values of the constant range from 100 to 900 cm^2·torr/s depending on the type of gas and ion.

The ambipolar diffusivity is obtained from an experimental determination of the rate of decay of the charged particle density in a cavity after the ionization source has been turned off. For this purpose, the particle number density is assumed to decay as $\exp(-t/t_r)$, where the decay constant t_r is the average lifetime of particles with respect to collision with the walls of a containing vessel. If the diffusion length appropriate for a given container is denoted by L, the ambipolar diffusivity is then given by

$$D_a = \frac{L^2}{t_r} \tag{10.14}$$

where the characteristic diffusion length L depends on the container geometry.

Example 10.1. The density of a charged particle, n, in a container decays according to $n = n_o \exp(-t/t_r)$. Here n_o is the density at the time the ionization source is turned off. Thus, a plot of ln n versus t yields the decay constant t_r. According to McDaniel (1964), the average collision lifetime, t_r, in a tube of 1 cm radius is 3×10^{-3} s at 1 torr of nitrogen and room temperature. The diffusion can be

described by

$$\frac{\partial n}{\partial t} = \nabla(D_a \nabla n) \tag{A}$$

If n decays in an exponential way, one can write

$$n = N(r, z)e^{-t/t_r} \tag{B}$$

For the cylindrical coordinate, Eq. (A) with Eq. (B) can be rewritten as

$$\frac{d^2N}{dr^2} + \frac{1}{r}\frac{dN}{dr} + \alpha^2 N = 0 \qquad \text{where } \alpha = \frac{1}{D_a t_r} \tag{C}$$

where it has been assumed that the tube is infinitely long. The boundary conditions are the symmetry around the center ($dN/dr = 0$) and vanishment of n at the wall or $N = 0$ at $r = r_o$. The solution to Eq. (C) is

$$N(r) = AJ_0(\alpha r) \tag{D}$$

with the condition

$$AJ_0(\alpha r_o) = 0 \tag{E}$$

where J_0 is the Bessel function of the first kind of order zero. There are many solutions to Eq. (E) and the first zero of J_0 occurs at $\alpha_1 r = 2.405$. If α_i is the ith root of J, one can write the solution as

$$n(r, t) = \sum_{i=1} A_i J_0(\alpha_i r)e^{-t/t_i} \tag{F}$$

According to Eq. (10.14) and the definition of α_i in Eq. (C), the diffusion length L, which in this case is dependent on the roots α_i, and thus L_i, is given by

$$\frac{1}{L_i^2} = \frac{1}{D_a t_i} = \alpha_i^2$$

The diffusion length corresponding to the first root is called fundamental or first mode and it is given by

$$\frac{1}{L_1^2} = \frac{1}{D_a t_1} = \left(\frac{2.405}{r_o}\right)^2 \tag{G}$$

The first mode is dominant after the time corresponding to t_1 and thus L (and therefore t_r) is taken as that for the first mode for the analysis of the data and the subsequent determination of D_a.

(*a*) Using only the fundamental mode, calculate the ambipolar diffusivity.

(*b*) Show that $t_2/t_1 = 0.19$ and thus experimental data for time larger than t_1 will give an accurate value of D_a.

Solution

(*a*) Since $r_o = 1$ cm, one has, from Eq. (G),

$$\frac{1}{D_a t_r} = 2.405^2$$

or

$$D_a = \frac{1}{2.405^2 t_r} = \frac{1}{2.405^2 \times 3 \times 10^{-3}} = 57.6 \text{ cm}^2/\text{s}$$

(*b*) The second root of Eq. (E) is given by $\alpha_2 r_o = 5.5$, or $\alpha_2 = 5.5$. The ratio, α_1/α_2, is given by

$$\frac{\alpha_1}{\alpha_2} = \left(\frac{D_a t_2}{D_a t_1}\right)^{1/2} = \left(\frac{t_2}{t_1}\right)^{1/2} = \frac{1}{2.29}$$

Thus, $t_2 = 0.19t_1$. Using only two terms in Eq. (F),

$$n(r, t) = A_1 J_0\left(\frac{2.405}{r_o}\right)e^{-t/t_1} + A_2 J_0\left(\frac{5.5}{r_o}\right)e^{-t/0.19t_1}$$

When $t = t_1$, the first term decays by e^{-1} or 0.37 but the second by $e^{-5.26}$ or 0.005. It is seen that for $t > t_1$, the first term is sufficiently accurate for the time dependence of n or for the plot of ln n versus t. The same value of D_a should result, regardless of the mode used.

The characteristic diffusion length is often used to describe a plasma. For simple geometries, these are (e.g., McDaniel, 1964)

$$L^2 = \begin{cases} \dfrac{1}{\pi^2(1/a^2 + 1/b^2 + 1/c^2)} & \text{rectangular channel of width } a, \text{ depth } b, \text{ and length } c \\ \left(\dfrac{r_o}{\pi}\right)^2 & \text{sphere of radius } r_o \\ \left[\left(\dfrac{2.405}{r_o}\right)^2 + \left(\dfrac{\pi}{H}\right)^2\right]^{-1} & \text{cylinder of radius } r_o \text{ and height } H \end{cases} \tag{10.15}$$

Example 10.2. According to Edelson and Flamm (1984), the major ion of interest for plasma etching based on CF_4 is CF_3^+. They give the following diffusivity for the ion:

$$D_i \text{ (cm}^2/\text{s)} = \frac{0.00146T_i^{1.75}}{P \text{ (torr)}}$$

For the plasma, they provide the following conditions:

$T_{gas} = 313$ K $\quad T_i = 453$ K $\quad T_e = 5.0$ eV $\quad$ (1 eV = 11,600 K)
Tube radius = 0.95 cm
Plasma length = 5 cm
$P = 0.5$ torr

Calculate the ion diffusivity and mobility. Obtain the ambipolar diffusivity. Calculate the characteristic diffusion length for the reactor and the average collision lifetime with reactor walls.

They also give the following conditions for the afterglow:

$T_g = T_i = 298$ K $\quad T_i = 0.025$ eV
Flow = 80 cm³/min (STP)

Calculate the distance down the tube after the plasma region at which the ion concentration reduces to 1 percent of the concentration in the plasma.

Solution. According to the expression for D_i,

$$D_i = \frac{0.00146(453)^{1.75}}{0.5}$$

$$= 130 \text{ cm}^2/\text{s}$$

Now the CF_3^+ ion mobility can be obtained from the Einstein relation [Eq. (10.7)]:

$$\mu_i = \frac{D_i q}{k_B T_i} = \frac{130}{8.62 \times 10^{-5} \times 453} = 3.33 \times 10^3 \text{ cm}^2/(\text{V}\cdot\text{s})$$

where $k_B = 8.62 \times 10^{-5}$ eV/K. From Eq. (10.13),

$$D_a = D_i \frac{T_e}{T_i} = 130 \frac{5 \times 11{,}600}{453} = 16{,}630 \text{ cm}^2/\text{s}$$

For the cylindrical tube of length 5 cm, one has, from Eq. (10.15),

$$L^2 = \frac{1}{(2.405/r_o)^2 + (\pi/H)^2}$$

$$= \frac{1}{(2.405/0.95)^2 + (3.14/5)^2}$$

$$= 0.147 \text{ cm}^2$$

Therefore, the characteristic diffusion length is 0.383 cm. The lifetime can be obtained from Eq. (10.14):

$$t_r = \frac{L^2}{D_a} = \frac{0.147}{16{,}640} = 8.8 \times 10^{-6} \text{ s}$$

The average fluid velocity v_f is

$$v_f = \frac{80 \times 760/0.5}{3.14 \times 0.95^2} = 42{,}910 \text{ cm/s}$$

Since the concentration decays on the average by the factor of t_r, one has

$$\frac{n}{n_0} = \exp\left(-\frac{t}{t_r}\right)$$

or

$$\ln\left(\frac{n}{n_0}\right) = -\frac{t}{t_r}$$

where n_0 is the concentration in the plasma. Thus,

$$\ln(0.01) = -\frac{t}{8.8} \times 10^{-6}$$

$$t = 4.05 \times 10^{-5} \text{ s}$$

The length l is therefore given by

$$l = tv_f = 4.05 \times 10^{-5} \times 42{,}910 = 1.74 \text{ cm}$$

Thus, the plasma is extinguished to 1 percent of the plasma strength in the afterglow by the time it travels 1.74 cm.

10.5 PLASMA CHARACTERISTICS AND ELECTRICAL PROPERTIES

As indicated in the introduction, relationships for plasma and its electrical properties are approximate. Furthermore, they are by no means applicable to all cases. It is with this understanding and caution that the relationships given in this section should be used.

A plasma can be characterized by its Debye length defined by

$$\lambda_D = \left(\frac{p_0 k_B T_e}{q^2 n_e}\right)^{1/2} \tag{10.16}$$

where p_0 is the permittivity of free space. An ionized medium cannot be called a plasma when its Debye length is longer than any surrounding dimensions of its boundary. The Debye length is a measure of sheath thickness. This arises from the fact that the plasma potential decays approximately with the factor of $\exp(-x/\lambda_D)$, where x is the distance from the electrode.

Since collisions by electrons cause ionization, a basic quantity in plasmas is the electron mean free path, λ_e, which is the mean distance an electron can travel without encountering a collision. If one lets f_e be the electron collision frequency, which is the number of collisions an electron experiences per unit time, the electron velocity v_e is given by

$$v_e = \lambda_e f_e \tag{10.17}$$

There are a number of constraints that a plasma system has to meet for breakdown (discharge) to occur and more importantly for efficient breakdown. It is obvious, for instance, that no breakdown will occur if the electron mean free path is larger than the electrode spacing d or the characteristic diffusion length L, since then all electrons vanish at container surfaces. For a dc discharge, the breakdown voltage is often correlated to Pd (pressure times diameter) for infinite parallel plates but more appropriately to PL (pressure times characteristic dimension) for an arbitrary container shape. According to the breakdown voltage presented by Brown (1966), the breakdown voltage increases abruptly for most gases when PL is less than 1 cm·torr. As the pressure and the dimension decrease, an enormous amount of energy is required to maintain the necessary amount of secondary electrons, which results in an abrupt change in the breakdown voltage. Therefore, a condition for an efficient dc discharge may be written as follows:

$$PL = \text{constant} \tag{10.18}$$

where the constant is around 4 cm·torr. The constant is that corresponding to the pressure at which the mean free path is about equal to the electrode separation. For ac (rf) discharge, an additional factor related to the frequency of the exciting field has to be taken into consideration, which in turn introduces a number of constraints. The electron collision frequency f_e has to be larger than the angular frequency of the external field, ω, to avoid the excessive breakdown voltage that

becomes necessary when the system goes through a transition from many collisions per oscillation of electron to many oscillations per collision. Another constraint is that the oscillation amplitude should be less than one half the characteristic diffusion length (one half the electrode spacing for infinite parallel plates) or else electrons can travel completely across the length and collide with the walls on every half-cycle. The combination of these constraints, including the mean free path constraint, that is, $L > \lambda_e$, leads to the following condition (Brown, 1966):

$$\frac{P^2 L}{\omega} = \text{constant} \tag{10.19}$$

where the constant is dependent on the external field applied. This condition is based on diffusion-controlled hydrogen plasma. Therefore, caution should be taken in applying it to other cases. Although the constants in Eqs. (10.18) and (10.19) are dependent on the plasma system, it is nevertheless very instructive to note that L or equivalently the electrode spacing is inversely proportional to P or P^2 for optimum breakdown voltage. This is the main reason why the electrode spacing is smaller for higher pressure plasmas. For example, for rf plasma systems at pressures higher than 1 torr the electrode spacing is typically less than 1 cm (Mathad, 1985).

Example 10.3. For hydrogen, the collision frequency is given (Brown, 1966) as follows:

$$f_e = 5.93 \times 10^9 P \text{ (torr)}$$

when the average electron energy is larger than a few electronvolts. Further, $P\lambda_e =$ 0.02 cm·torr for the average electron energy of 5 volts. Let m be the electron mass (9.1×10^{-28} g). Then

$$v_e^2 = \frac{8 k_B T_e}{\pi m} \tag{A}$$

Calculate the electron temperature.

Solution. The velocity is given by Eq. (10.17):

$$v_e = f_e \lambda_e = 5.93 \times 10^9 P \frac{0.02}{P} = 1.19 \times 10^8 \text{ cm/s}$$

From Eq. (A),

$$T_e = \frac{\pi m v_e^2}{8 k_B} = \frac{3.14 \times 9.1 \times 10^{-28} \times (1.19 \times 10^8)^2}{8 \times 1.38 \times 10^{-6}} = 3.7 \times 10^4 \text{ K}$$

Example 10.4. For the CF_4 plasma in Example 10.2, determine the constant in Eq. (10.19) assuming that they used the typical frequency of 13.56 MHz and that the constant evaluated in this way can be applied to the plasma system so long as the applied voltage does not change significantly around the value used in the experiment. Based on the result, calculate the characteristic diffusion length required for

efficient ignition of plasma when the angular frequency changes from 13.56 to 3.0 MHz.

Solution. Since the frequency is equal to $2\pi\omega$, one has

$$13.56 \times 10^6 = 2\pi\omega$$

$$\omega = 2.16 \times 10^6$$

From Example 10.2, $L = 0.383$ cm and $P = 0.5$ torr. Thus,

$$\frac{P^2 L}{\omega} = \frac{0.5^2 \times 0.383}{2.16 \times 10^6}$$

$$= 4.43 \times 10^{-8} \text{ torr}^2\text{·cm/s}$$

Thus, the criterion under the assumptions can be written as

$$\frac{P^2 L}{\omega} = 4.43 \times 10^{-8} \text{ torr}^2\text{·cm/s} \tag{A}$$

When the angular frequency changes to 3.0 MHz, it has to satisfy Eq. (A):

$$L = \frac{4.43 \times 10^{-3}\omega}{P^2}$$

$$= \frac{4.43 \times 10^{-8} \times 3.0 \times 10^6/6.28}{0.25}$$

$$= 0.085 \text{ cm}$$

This length is too small to be practical.

Another quantity that characterizes a plasma is plasma frequency. It is the angular frequency with which the plasma will oscillate around its equilibrium position and is given by

$$\omega_p^2 = \frac{q^2 n_e}{m p_0} \tag{10.20}$$

where ω_p is the plasma frequency. In the sheath where the charge carriers are mainly ions, an equivalent quantity is "ion" frequency $(\omega_p)_i$, which can be defined the same way as with ω_p but with n_e and m_e replaced by n_i and M_i, respectively. An ac (rf) plasma system is often modeled as an equivalent electrical circuit for electrical characterization. The plasma frequency can be used to determine whether sheath and plasma can be treated as a resistor or a capacitor in the equivalent circuit. Although it is still subject to dispute, the following conditions due to Zarowin (1983) could be useful:

$$\omega \gg \frac{\omega_p^2}{f} \quad \text{(capacitive)}$$
$$\omega \ll \frac{\omega_p^2}{f} \quad \text{(resistive)} \tag{10.21}$$

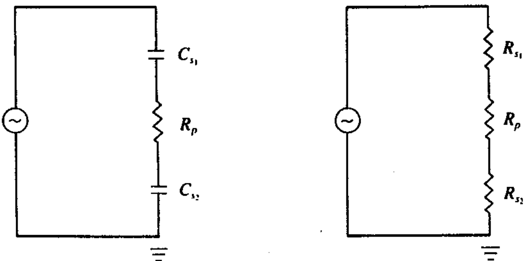

FIGURE 10-9
Equivalent circuit representation of plasma system (Zarowin, 1983).

It is understood in Eq. (10.21) that ω_p and f are $(\omega_p)_e$ and f_e for the plasma and they are $(\omega_p)_i$ and f_i for the sheath where f_i is the collision frequency of ions with neutrals in the sheath. The two equivalent circuits are shown in Fig. 10-9. According to Zarowin, the usual resistive plasma and capacitive sheaths result when

$$2.5\text{ MHz} < \frac{\omega}{2\pi} < 65\text{ MHz} \tag{10.22}$$

Example 10.5. Typical plasma-etching conditions are given (Zarowin, 1983) below:

$$n_e = 10^{10}\text{ cm}^{-3} \qquad f_e = 7 \times 10^{10}\text{ s}^{-1} \qquad f_i = 2 \times 10^{-7}\text{ s}^{-1}$$
$$n_i = 10^{10}\text{ cm}^{-3} \qquad M = 10^5\text{ m}$$

Show for the typical rf frequency of 13.56 MHz that the plasma is resistive and the sheath is capacitive according to the criteria of Eq. (10.21). Note that $p_0 = 8.85 \times 10^{-12}\text{ C}^2/(\text{N}\cdot\text{m}^2)$ and $q = 1.6 \times 10^{-19}$ C/electron.

Solution. For the plasma, Eq. (10.20) can be used:

$$\omega_p^2 = \frac{q^2 n_e}{m p_0}$$
$$= \frac{(1.6 \times 10^{-19})^2}{(9.1 \times 10^{-31})(8.85 \times 10^{-12})} n_e$$
$$= 3179 n_e \qquad (\text{m}^3/\text{s})$$

or

$$\omega_p = 56{,}380 n_e^{1/2} \qquad (n_e \text{ in cm}^{-3})$$
$$= 5.64 \times 10^9\text{ s}^{-1}$$

Thus, one has, for $f_e = 7 \times 10^{10}\text{ s}^{-1}$,

$$\frac{\omega_p^2}{f_e} = \frac{(5.64 \times 10^9)^2}{7 \times 10^{10}} = 4.54 \times 10^8\text{ s}^{-1} \tag{A}$$

For the excitation frequency, the angular frequency is

$$\omega = 2\pi \times 13.56 \times 10^6 = 8.52 \times 10^7\text{ s}^{-1} \tag{B}$$

From Eqs. (A) and (B) and Eq. (10.21), it can be concluded that the plasma is resistive.

For the sheath,

$$(\omega_p)_i = \frac{q^2 n_i}{M p_0} = \omega_p \left(\frac{m}{M}\right)^{1/2} \left(\frac{n_i}{n_e}\right)^{1/2}$$
$$= 5.64 \times 10^9 (10^{-5})^{1/2} (1)^{1/2}$$
$$= 1.78 \times 10^7\text{ s}^{-1}$$
$$\frac{(\omega_p)_i^2}{f_i} = \frac{(1.78 \times 10^7)^2}{2} \times 10^7$$
$$= 1.58 \times 10^7 \tag{C}$$

Equations (B) and (C) show that the sheath is capacitive according to the criteria of Eq. (10.21).

The most prominent quantity in characterizing a plasma is the electron collision frequency or, equivalently, the mean free path. The collision frequency can be written as

$$f_e = Q_c n_0 v_e \tag{10.23}$$

where n_0 is the number density of neutrals, v_e is the electron velocity, and Q_c is called the collision cross section, which is a measure of the probability of collision between electrons and neutrals. The reason that the collision frequency cannot be readily determined is the strong nonlinear dependence of the collision cross section on the applied voltage. It is also strongly dependent on the type of gas molecules. Furthermore, many basic quantities required to characterize a plasma such as electron temperature cannot be measured directly, but must be inferred from electrical measurements. This is much more of a problem for ac discharges than for dc discharges.

Consider the simpler case of dc discharges. For deposition by physical sputtering, which is of major interest for dc discharges, the rate of sputtering is that given by Eq. (9.13). All quantities of interest can be determined from the measurements of voltage and current at the cathode. The requirement of eliminating plasma formation in the spacing between the target and ground shield can be satisfied by insisting that the sheath thickness corresponding to the cathode potential be smaller than the spacing. This gives a conservative value since the cathode potential is the highest in the container and thus the thickness is the

maximum possible. This sheath thickness is that given by Eq. (9.14):

$$d^2 = \frac{0.85 p_0 q^{1/2} V_{sp}^{3/2}}{j_i M_i^{1/2}} \tag{10.24}$$

where V_{sp} is the cathode (sheath) potential, d is the sheath thickness, and j_i is the ion current density.

For ac discharges, two quantities that can be determined from electrical measurements have already been given in Chap. 9 (refer to Fig. 9-10):

$$V_p = 0.5(V_a + V_{dc}) \tag{10.25}$$

$$V_{sp} = V_p - V_{dc} \tag{10.26}$$

where V_a is the applied excitation voltage, V_{dc} is the corresponding dc bias, V_{sp} is the sheath potential, and V_p is the plasma potential. Measurement of the average (rms) current I_r yields the sheath current density (flux) at the powered electrode, J_{sp}:

$$J_{sp} = \frac{I_r}{A_p} \tag{10.27}$$

where A_p is the area of the powered electrode.

In rf discharges, the maximum power dissipation in the discharge occurs when the impedance of the external circuit is matched to the internal (discharge) impedance. Under this condition, and in the excitation frequency range given by Eq. (10.23) corresponding to the capacitive circuit model in Fig. 10-9, the sheath electric field E_{sp} is given by (Zarowin, 1983)

$$E_{sp} = \frac{J_{sp}}{\omega p_0} \tag{10.28}$$

It follows then that the sheath thickness (powered side) d_{sp} is given by

$$d_{sp} = \frac{V_{sp}}{E_{sp}} \tag{10.29}$$

where a linear voltage drop across the sheath has been assumed. Note that $d_{sp} = d_p$ and $V_{sp} = V_p$ when the powered electrode area is the same as the grounded electrode area.

The electron temperature can then be estimated from Eq. (9.18):

$$V_p - V_f = \frac{k_B T_e}{2q} \ln\left(\frac{M}{2.3m}\right) \tag{10.30}$$

where V_f is the floating potential with respect to a ground for a substrate (probe) immersed in a plasma.

Example 10.6. From the data and results given in Example 9.4, calculate the spacing between the target and ground shield required to eliminate plasma formation in the space.

Solution. From Example 9.4,

$$V_{sp} = 850 \text{ volts} = 850 \text{ kg·m}^2/(\text{s}^2\text{·C})$$

$$j_i = 2.27 \times 10^{-4} \text{ A/cm}^2 = 2.27 \times 10^{-4} \text{ C/(s·cm}^2)$$

Also, $q = 1.6 \times 10^{-19}$ C, $M = 0.018$ kg for Ar and $p_0 = 8.85 \times 10^{-12}$ C^2·s^2/(kg·m^3). Therefore, Eq. (10.22) yields

$$d^2 = \frac{0.85 \times (8.85 \times 10^{-12})(1.6 \times 10^{-19})^{1/2}(850)^{3/2}}{(2.27 \times 10^{-4})(0.018)^{1/2}}$$

$$= 2.45 \times 10^{-12} \text{ cm}^2$$

or

$$d < 1.57 \times 10^{-6} \text{ cm}$$

It is seen that the ground shield in Fig. 10-5 should literally touch the target under the conditions.

Example 10.7. For an asymmetrical, parallel-plate rf discharge operating at 13.56 MHz, the root mean square current and applied voltage amplitude determined from electrical measurements are 0.1 A and 160 V, respectively. The dc bias with respect to the ground is (−40) V. The powered electrode area is 10 cm^2 and the grounded electrode area is 30 cm^2. For Ar plasma, suppose that the use of the probe shown in Fig. 10-10 with equal area electrodes yields a floating potential of 10 V with respect to the ground. Determine the following: V_p, V_{sp}, J_{sp}, d_{sp}, T_e, v_e, and the ion fluxes at both electrodes, assuming that ion collisions in the sheath are negligible.

Solution. From Eqs. (10.25) through (10.27), one has

$$V_p = 0.5(160 - 80) = 40 \text{ V}$$

$$V_{sp} = V_p - V_{dc} = 40 - (-40) = 80 \text{ V}$$

$$J_{sp} = \frac{I_r}{A_p} = \frac{0.1}{10} = 0.01 \text{ A/cm}^2$$

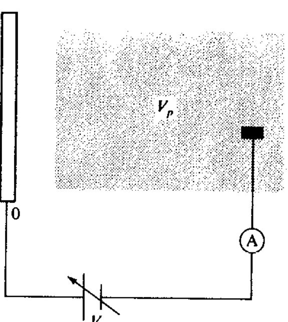

FIGURE 10-10
Schematic for probe measurements in a plasma (Chapman, 1980).

From Eqs. (10.28) and (10.29),

$$E_{sp} = \frac{J_{sp}}{\omega p_0}$$
$$= \frac{0.01 \times 10^4}{(2\pi \times 13.56 \times 10^6)(8.85 \times 10^{-12})}$$
$$= 1.31 \times 10^5 \text{ (s·A·N/C}^2\text{)}$$
$$= 1.31 \times 10^5 \text{ (N/C)} = 1.31 \times 10^5 \text{ V/m}$$

Thus,

$$d_{sp} = \frac{80}{1.31 \times 10^5} = 0.61 \times 10^{-3} \text{ m}$$

From Eq. (10.30),

$$V_p - V_f = 30 = \frac{k_B T_e}{2q} \ln\left(\frac{M}{2.3m}\right) = \frac{k_B T_e}{2q} \ln\left(\frac{18/6 \times 10^{23}}{2.3 \times 9.1 \times 10^{-28}}\right)$$
$$= 4.78\left(\frac{k_B T_e}{q}\right)$$

or

$$\frac{k_B T_e}{q} = \frac{30}{4.78} = 8.36 \text{ V}$$

Thus, the electron temperature is that corresponding to 8.36 eV or 97,000 K. For the electron velocity, Eq. (A) in Example 10.3 can be used:

$$v_e = \left(\frac{8k_B T_e}{\pi m}\right)^{1/2}$$
$$= \left(\frac{8 \times 1.38 \times 10^{-16} \times 97{,}000}{3.14 \times 9.1 \times 10^{-28}}\right)^{1/2} = 1.94 \times 10^8 \text{ cm/s}$$

The ion flux at the powered electrode is very close to that corresponding to J_{sp} [see Eq. (10.27)]. Thus,

$$j_{sp} = \frac{J_{sp}}{q} = \frac{0.01}{1.6 \times 10^{-19}} = 6.18 \times 10^{16} \text{ cm}^{-2}\text{·s}^{-1}$$

To calculate the ion flux, the fact that the current must be the same at both electrodes is used:

$$J_{sp} A_p = J_g A_g$$

Thus,

$$j_g = \frac{j_{sp} A_p}{A_g} = 6.18 \times 10^{16} \times 10/30 = 2.06 \times 10^{16} \text{ cm}^{-2}\text{·s}^{-1}$$

Example 10.8. Suppose that ambipolar diffusion experiments yield a D_a of 16,000 cm^2/s and a collision lifetime (time between collisions) of 8.8×10^{-14} s, when the same apparatus as in Example 10.7 is used. Based on the data here and those in Example 10.7, calculate μ_i and n_e. Also calculate the electron collision cross section. Assume the pressure is 0.5 torr and the plasma gas temperature is 300 K.

Use the following relationships:

$$J_p = \frac{C_d V_p}{H} \quad \text{(A)}$$

$$C_d = \frac{n_e q^2}{m f_e} \quad \text{(B)}$$

where C_d is the plasma conductivity and H is the electrode separation, which is 5 cm for this example.

Solution. The ion mobility can be obtained from Eq. (10.12):

$$\mu_i = \frac{q}{k_B T_e} D_a$$
$$= \frac{1}{(8.62 \times 10^{-5})(97{,}000)} (16{,}000) = 1.91 \times 10^3 \text{ cm}^2/(\text{V·s})$$

where $k_B = 8.62 \times 10^{-5}$ eV/K. The collision lifetime is the inverse of the collision frequency. One has, from Eq. (10.23),

$$Q_c = \frac{f_e}{n_0 v_e} = \frac{1}{t_r n_0 v_e}$$

The number density of neutrals n_0 can be obtained from the ideal gas law:

$$n_0 = \frac{P}{k_B T} = \frac{(0.5/760)(6 \times 10^{23})}{82 \times 300} = 1.6 \times 10^{16} \text{ cm}^{-3}$$

Therefore,

$$Q_c = \frac{1}{(8.8 \times 10^{-14})(1.6 \times 10^{16})(1.94 \times 10^8)} = 3.66 \times 10^{-12} \text{ cm}^2$$

From Eq. (A), the conductivity C_d is

$$C_d = \frac{HJ_p}{V_p} = \frac{0.03 \times 0.05}{40} = 3.75 \times 10^{-5} \ \Omega^{-1}\text{·m}^{-1}$$

From Eq. (B),

$$n_e = \frac{C_d m f_e}{q^2} = \frac{C_d m}{t_r q^2} = \frac{(3.75 \times 10^{-5})(9.1 \times 10^{-31})}{(8.8 \times 10^{-14})(1.6 \times 10^{-19})^2}$$
$$= 1.51 \times 10^{16} \text{ m}^{-3} = 1.51 \times 10^{10} \text{ cm}^{-3}$$

The above examples should reveal that most of the quantities of interest for plasma processing can be determined on the basis of electrical measurements and ambipolar diffusion experiments. However, these quantities are applicable only to the set of conditions under which the measurements are made. Therefore, for

predictability, plasma characteristics have to be related to plasma design and operating conditions. These are: applied voltage, electrode areas, pressure, and reactor geometry for a given excitation frequency. A quantity representing the reactor geometry is the characteristic diffusion length. As was evident in Example 10.7, the electrode area ratio is another quantity that can be used to interpret plasma characteristics. The plasma electric field E_p is a measure of energy per unit distance over the potential. Further, pressure is a measure of the number of particles per unit volume. Thus, E_p/P is often used to represent plasma characteristics. Numerous examples of the use of E_p/P can be found, for example, in Brown (1966).

Another quantity often used in correlations for plasma characteristics is PL. This quantity can be viewed from the point of degree of ionization. If a beam of current i_0 is injected into a medium with a neutral number density N in a vessel with a characteristic diffusion length L, then the degree of ionization α, which can be defined as i_i/i_0, is given (McDaniel, 1964) by

$$\alpha = Q_i N L \tag{10.31}$$

where the ionization collision cross section Q_i can be expressed in terms of the collision probability P_i as follows:

$$Q_i = 0.283 \times 10^{-16} P_i \tag{10.32}$$

The probability P_i is in turn dependent on electron energy. As shown in Fig. 10-11, the probability increases almost linearly with electron energy and then goes through a maximum at around 90 eV. The probability is almost zero below

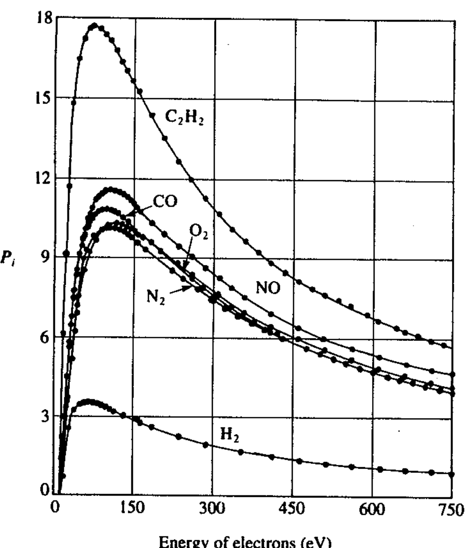

FIGURE 10-11
Collision probability for a number of gases (McDaniel, 1964).

a certain energy level, which is required to activate neutrals into ions. Note in this regard that N is proportional to P.

There are presently no *a priori* methods of relating the plasma characteristics to plasma operating and design conditions. The alternative is to correlate the plasma characteristics of interest to E_p/P and PL for a given plasma system through experiments. These results, in turn, can be used to describe or design a plasma reactor.

10.6 INTRINSIC KINETICS AND PLASMA AND TRANSPORT EFFECTS

There are two aspects unique to plasma deposition and etching. The first is that the rate constants in the intrinsic kinetics are dependent on ion energy (and ion flux) since the surface modification by ions is the major source of enhancement in the deposition and etching. The second is that, for ions, the transport effects are confined to the plasma sheath. The transport of active neutrals, which are responsible for the deposition or etching, is not restricted to the sheath but is operative throughout the reactor, as was the case in the conventional CVD.

Unlike the kinetics of conventional CVD, the intrinsic kinetics have to account for the enhancement caused by ion surface modification. The surface modification is mainly by momentum transfer with the colliding ions. Since the degree of modification is dependent on the ion energy, the activation energy in turn depends on the ion energy. The ion flux, on the other hand, determines the fraction of the substrate surface affected by the ion bombardment. One would expect that more than one site of the surface is affected per incident ion. However, if the ion flux is not sufficiently high, only a fraction of the surface would be affected. One would also expect the ion flux to have a small effect beyond a certain ion flux at which the whole surface is affected. This ion flux may be termed the critical ion flux. Therefore, all rate constants in the intrinsic kinetics are dependent not only on the ion flux but also on the ion energy after reaching the critical ion flux. Plasma reactors are usually designed and operated so as to increase the ion flux.

Therefore it is necessary to relate the rate constants to ion energy and ion flux after extracting intrinsic kinetic information from observed rates. With respect to transport effects, the buoyancy (free convection) effect is negligible due to low-temperature processing. As will be discussed shortly, the velocity profiles are well defined for a reactor that can be used to generate intrinsic kinetics. Thus, it is sufficient to consider only the mass transfer effect for the reactive neutral species of interest.

A criterion is available that can be used to determine whether or not the experimental data are free from the mass transfer effect. In conventional CVD, the concentration readily measurable via a sampling line is the bulk concentration. In plasma reactors, on the other hand, there can be two different concentrations that are relevant to the plasma processing: the bulk concentration if the sampling is directly from inside the plasma and the local concentration in the

plasma. The point here is that any concentration measurement from outside the plasma does not represent the concentration of interest since the reactive neutrals can readily recombine outside the plasma. While the local concentrations can be measured readily, measurement of the bulk concentration would depend on reactor configuration. Therefore, the mass transfer coefficient for active neutral species, k_m, is defined as follows:

$$R_G = k_m(C_p - C_s) \tag{10.33}$$

where R_G is the observed rate of etching or deposition per unit area, C_p is the species concentration at the electrode opposite to the one where substrate is placed, and C_s is the surface concentration of the species at the substrate. Since the temperature gradient in plasma, and thus the mass flux due to the temperature gradient, is negligible, one can write

$$R_G = D \left.\frac{\partial C}{\partial y}\right|_0 \tag{10.34}$$

It can be shown from Eqs. (10.33) and (10.34) (see Prob. 10.15) that the Sherwood number is given by

$$\text{Sh} = \frac{k_m H}{D} = \begin{cases} 2 & \text{(no flux condition)} \\ 1 & \text{(constant wall concentration condition)} \end{cases} \tag{10.35}$$

where H is the electrode separation. The first is for the case where there is no consumption of the neutral species at the electrode opposite to the substrate electrode, which would be typical of plasma reactors. For the experimental reactors considered in this section, the concentration at the electrode opposite to the substrate electrode is kept constant. In this case, the Sherwood number of unity is used for the mass transfer coefficient. If the bulk concentration is to be used, the Nusselt numbers are

$$\text{Sh} = \begin{cases} \dfrac{20}{7} & \text{(no flux condition)} \\ 1 & \text{(constant wall concentration condition)} \end{cases} \tag{10.36}$$

One can readily determine whether the experimental data obtained are intrinsic or not on the basis of the mass transfer coefficient and the observed rate. As was the case in Chap. 6, this can be determined by calculating the magnitude of the following:

$$W = \frac{R_G H}{\text{Sh}\, D C_i} \qquad \text{for } i = b, p \tag{10.37}$$

where the subscripts b and p, respectively, are for the concentration in the bulk fluid and that in the fluid near the top wall.

Since the ratio W is equal to $(1 - C_s/C_p)$, which follows from Eq. (10.33), a W value close to unity means that the observed rate is severely affected by mass transfer resistance; a value close to zero means that the rate is almost unaffected

by mass transfer limitations. Although one may conclude that plasma processing is typically free from mass transfer effects due to the high diffusivity (100 cm^2/s and higher) of neutrals at the low pressures (at most, 10 torr) typically employed, one should take note of the fact that the ratio W represents the relative magnitude of two rates. Thus, the relative rates and not the absolute values determine the extent to which the observed rate is affected by diffusion.

Example 10.9. In plasma etching in CF_4, fluorine atoms are the reactive neutral species. It is believed that the same is true in plasma etching in NF_3. For NF_3, Stenger *et al.* (1987) give the following conditions:

Etch rate = 0.15 μm/min	$T = 25°C$	$P = 40$ Pa (0.3 torr)
Inlet mole fraction of NF_3 = 0.4		Inlet flow rate = 25 sccm
Electrode separation = 1.5 cm		$D_F = 680\ cm^2/s$

Determine whether the kinetic data obtained under these conditions are affected by mass transfer resistance. Note in this regard that the use of NF_4 (as opposed to CF_4) does not lead to polymer formation. The intrinsic etching rate is first order with respect to F and the rate constant is 23.5 cm/s (Stenger *et al.*, 1987). Calculate the fraction of neutral F atoms in the plasma. Determine the electron density in the plasma assuming that all the rate constants involved are known. Assume for this part that the reactor is a simple planar reactor with symmetrical electrodes of 100 cm^2 and with no radial flow, i.e., flow in the direction parallel to the electrodes.

Solution. The etch rate can be calculated as follows:

$$R_G = \frac{\rho G}{M} = \frac{2.33 \times (0.2 \times 10^{-4}/60)}{28.1} = 2.764 \times 10^{-8}\ \text{mol/(cm}^2\cdot\text{s)}$$

where M and ρ are the silicon atomic weight and density, respectively, and G is the linear (centimeters per second) etch rate. From the ideal gas law, the concentration of NF_4 is

$$C = \frac{p_i}{R_g T} = \frac{(0.3/760) \times 0.4}{82 \times 298} = 6.46 \times 10^{-9}$$

If the etch rate is first order with respect to F atoms and the rate constant is 23.5 cm/s, the fluorine atom concentration [F] is

$$[\text{F}] = \frac{R_G}{k} = \frac{2.764 \times 10^{-8}}{23.5} = 1.176 \times 10^{-9}\ \text{mol/cm}^3$$

Thus, the fraction of F atoms in the plasma f is

$$f = \frac{[\text{F}]}{C_t} = \frac{1.176 \times 10^{-9}}{6.46 \times 10^{-9}/0.4} = 0.073$$

where C_t is the concentration of all species in the plasma (note in this regard that concentrations of electrons and ions are negligible). According to the criterion of Eq. (10.37), one has

$$W = \frac{2.764 \times 10^{-8} \times 1.5}{\text{Nu}_m 680 \times 1.176 \times 10^{-9}} = \frac{0.052}{\text{Nu}_m} = \frac{0.052}{20/7} = 0.018$$

The ratio W in this case is $(1 - C_s/C_b)$. Thus, the data are almost free from mass transfer effects.

For part two, a steady-state balance for F atoms can be used:

$$\text{In} + \text{generation} = \text{out} + \text{consumption}$$

$$0 + v_p k_g n_e[\mathrm{NF_3}] = Q[\mathrm{F}] + k_1[\mathrm{F}]A + k_2[\mathrm{F}]v_p$$

where Q is the volumetric flow rate, A is the substrate area, v_p is the plasma volume, n_e is the electron concentration, and k_g, k_1, and k_2 are rate constants. Thus, the electron concentration is given by

$$n_e = \frac{[\mathrm{F}](Q + k_1 A + k_2 v_p)}{k_g[\mathrm{NF_3}]v_p}$$

One unique aspect of plasma kinetics is that a change in pressure causes not only a change in the concentration but also a change in the rate constants involved. Therefore, intrinsic data obtained at one pressure cannot be related to data at another pressure, even if all the other conditions remain the same, unless proper corrections are made. This is due to the fact that a pressure change also brings about changes in plasma characteristics, which in turn changes ion flux, ion energy, and the concentration of reactive neutral species, beyond the change expected from the pressure effect on concentration.

To examine how one can make a change in concentration without affecting the ion energy for given power input and rf frequency, examine the plasma and sheath (powered electrode) potentials. Depending on where the substrate is placed, one of the two potentials determines the ion energy, although some consideration should be given to the energy loss in the sheath due to collisions. When pressure is very low, the collision frequency of ions with neutrals is very low such that the potential is equivalent to the ion energy, as in a dc discharge. When the pressure is relatively high such that the mean free path of ions is not much larger than the sheath thickness, the potential is not equivalent to the ion energy. The probability of having no collision in travelling a distance x is given by $\exp(-x/\lambda)$, where λ is the mean free path (e.g., Chapman, 1980). The probability of having no collision in traveling the sheath thickness d, P_d, is therefore given by

$$P_d = \exp\left(-\frac{d}{\lambda}\right) \tag{10.38}$$

where the mean free path of ions in neutrals (McDaniel, 1964) is given by

$$\lambda = \left[\pi n_i d_i^2 (2)^{1/2} + \pi n_n \left(\frac{d_i + d_n^2}{2}\right)^{1/2} \left(1 + \frac{M_i}{M_n}\right)^{1/2}\right]^{-1} \tag{10.39}$$

The relationship gives good order of magnitude agreement with experiments for the slightly ionized gases, typical of plasma processing. Here n is the number density, d is the molecular diameter, M is the molecular weight, and the subscripts i and n, respectively, are for ions and neutrals. The mean free path

decreases with increasing pressure. The sheath thickness also decreases with increasing pressure but at a much lower rate. Thus, as the pressure decreases, d/λ decreases and the probability of having no collision [Eq. (10.38)] approaches unity.

As apparent from Eq. (10.38), the probability of collision in the sheath approaches zero when d/λ is much less than unity, which occurs when the pressure is low, say less than 0.01 torr, as in a typical dc discharge. Thus, the sheath potential itself is the ion energy. In the other extreme case in which the sheath thickness is large relative to the mean free path, the average ion energy E_i (Davis and Vanderslice, 1963) is given by

$$E_i = \lambda_i q E_j \qquad \text{for } j = p \text{ or } sp \tag{10.40}$$

where E_j is the electric field for plasma or sheath. Note that the ion energy is proportional to E_j/P, since the mean free path is inversely proportional to pressure. Thus, the ion energy is the same if E_j/P is the same. The ion flux can be determined from the measured root mean square (rms) current although both electrons and ions contribute to the current in alternating frequencies (see Prob. 10.17 for a relationship for the ion flux). The ion flux is less than the current flux (density), but it is nevertheless proportional to the current density.

There are no universal relationships for E_j/P. Nevertheless, it is known that it can be correlated to PL and that at least in the regime where efficient ignition of plasma takes place [satisfying the condition of Eq. (10.18) for a dc discharge or that of Eq. (10.19) for an rf discharge], E_j/P is a monotonic function of PL: there is one and only one value of E_j/P for a given value of PL. This means that each time a pressure change is made in an experimental reactor, the characteristic diffusion length or the electrode spacing has to be changed to get experimental data for the same ion energy and thus the same rate constants, at least with a saturated ion flux. Therefore, it is necessary to establish experimentally a relationship between E_j/P and PL prior to kinetic experiments.

Example 10.10. For argon plasma with asymmetrical electrodes, Song (1988) gives the data in Fig. 10-12. The ranges of variables for the data are: 0.03 to 0.9 torr, 0.08 to 0.73 W/cm^2 power density, and electrode separation of 2 to 5 cm. For this example, however, suppose that the data are for symmetrical electrodes. Calculate the electrode separation required for 0.2 torr that will yield the same ion energy as that for 0.50 torr and electrode separation of 2 cm. The reactor is a quartz cylinder with a diameter of 10 cm and the electrodes are on the top and bottom of the cylinder.

Solution. For the reference conditions of 0.7 torr and 2 cm, one has, from Eq. (10.15),

$$\lambda_r = \left[\frac{1}{(2.405/5)^2 + 9.86/H^2}\right]^{1/2} = 0.61 \text{ cm} \tag{A}$$

Since $P = 0.5$ torr and $(PL)_r = 0.305$ cm·torr, the value of E_p/P corresponding to the value of PL in Fig. 10-12 is 30 V/(cm·torr). For the ion energy to be the same, E_p/P should remain the same. This in turn means that PL should be the same. Thus,

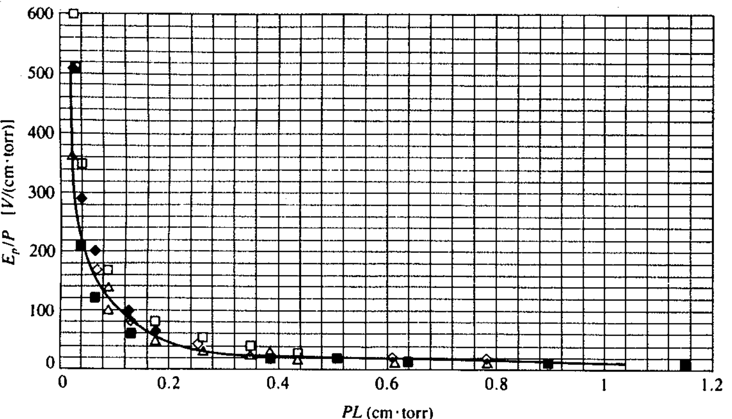

FIGURE 10-12
PL versus E_p/P (Song, 1988).

$PL = 0.305$. Solving this for L for 0.2 torr yields

$$L = \frac{0.305}{0.2} = 1.525 \text{ cm}$$

From Eq. (10.15),

$$1.525 = \left[\frac{1}{(2.405/5)^2 + 9.86/H^2}\right]^{1/2}$$

Solving this for H yields 6.98 cm.

As illustrated in the above example, kinetic data at various pressures (concentrations) but at the same ion bombardment energy can be obtained. There remain two items that must be resolved for the use of the data for intrinsic kinetics. The first is to properly account for mass transfer resistance, if any. The second has to do with the proper way of representing the effects of ion energy and ion flux on the rate. As discussed earlier in this section, the ion energy is a measure of the extent to which the activation energy is reduced by surface modification by colliding ions. Therefore, the activation energy is dependent on the ion energy. The ion flux is a measure of the fraction of the substrate surface affected by the colliding ions. Above a certain saturation value of the ion flux, any further increase should have negligible effects for a given ion energy. In analogy with the change of heat of adsorption with surface coverage for heterogeneous surfaces, one may postulate the following for the change of the activation energy E_a:

$$E_a = E_o - \frac{AJ_p}{1 + AJ_p} g[E_i] \tag{10.41}$$

where A is a constant representing the extent to which the ion flux approaches the saturation, E_o is the activation energy in the absence of ions, and g is a function representing the effect of the ion energy, E_i. It is noted that E_o can be determined by independent experiment. Although J_p is not the ion flux, it can be used as such since the ion flux is proportional to J_p and the proportionality constant can be absorbed into the constant A.

In general, intrinsic kinetics can be written as follows:

$$r_c = kf(C) \tag{10.42}$$

where r_c is the intrinsic rate, k is the rate constant, and $f(C)$ represents the concentration dependence. The rate constant, k, in plasma etching or deposition can be written in the following form with the aid of Eq. (10.41):

$$k = k_o \exp\left[\left(-E_o + \frac{AJ_p g}{1 + AJ_p}\right)\left(\frac{1}{R_g T}\right)\right] \tag{10.43}$$

where k_o is the preexponential factor and R_g is the gas constant. If the concentration dependence $f(C)$ is assumed for the determination of intrinsic kinetics from experimental data, the observed rate, R_G, is that given by

$$R_G = k_s f(C_s) \tag{10.44}$$

where the subscript s denotes evaluation of the quantity at the substrate surface. If first-order kinetics is assumed, as in Example 10.8, $r_c = k_s C_s$. The value of k_s is the rate constant at the substrate temperature; C_s can be determined from Eqs. (10.33) and (10.34) or Eq. (10.36). From the measured values of R_G and C_p(or C_b), the rate constant can be determined for an assumed form of $f(C_s)$, as illustrated in Chap. 5. The rate constant thus determined may be related to ion energy and ion flux in the form suggested by Eq. (10.43).

Since the intrinsic kinetics for etching or deposition involve the concentration of reactive neutral species, it is necessary to determine the homogeneous kinetics of the reactions leading to the formation of the neutral species. One complication with the homogeneous reactions is the formation of polymers and its deposition on the walls. For intrinsic kinetics, however, all that is required is steady state, i.e., constant reactive species concentration in the plasma. The steady-state concentrations can be used for the kinetics since an equilibrium exists between the wall polymer concentration and the neutral species concentration after the steady state is reached (Edelson and Flamm, 1984). A balance for the reactive neutral species for a flow-through reactor is

$$v_p r_G = QC_n + R_G A_s \tag{10.45}$$

where r_G is the net rate of generation of the reactive species, Q is the volumetric flow rate, C_n is the concentration of the reactive species exiting the plasma, and A_s is the substrate surface area. Since all quantities in the right-hand side of Eq. (10.45) are known, the net rate of generation can be determined from the measurements. The net rate of generation consists of the rate of generation of the reactive species and the rate of consumption due to recombination. Each rate

process can be considered elementary and thus the rates can readily be written provided the major reactions are known. The rate of generation r_g in general can be written as

$$r_g = k_g n_e C_m = k'_g n_e n_m \tag{10.46}$$

where k_g is the rate constant and C_m is the concentration of the main neutral species in the plasma. For CF_4 plasma, for example, the concentration is that of CF_4. Depending on the recombination routes, the rate of consumption by recombination can be complicated. However, for CF_4 plasma, it appears that the main path is by recombination among the neutral F atoms (Edelson and Flamm, 1984), in which case the rate of recombination r_r can be written as $k_r C_F^2$. The electron concentration or the number density can be inferred from the fact that the plasma conductance, at least in the range of electron density of interest (10^9 to 10^{12} cm^{-3}), is proportional to the electron concentration. Thus, Eq. (10.46) is rewritten with the aid of Eq. (A) in Example 10.8 as follows:

$$r_g = k_G\left(\frac{HJ_p}{V_p}\right)C_m \qquad \text{where } k_G = k_g \alpha_g \tag{10.47}$$

and α_g is the proportionality constant. Given measurements of C_n, J_p and V_p, and C_m from the ideal gas law, the rate constants can be determined with the aid of Eq. (10.45) and the recombination rate.

An experimental reactor suitable for the determination of intrinsic kinetics is shown in Fig. 10-13, which is the same as that used by Song (1988) except that it has symmetrical electrodes. The gas is fed through a quartz distributor which is circular with a perforated bottom such that the gas is distributed onto the substrate located on the powered electrode, and then exits to the vacuum pump via the annulus formed by the distributor and the outside quartz walls. A ground shield is placed in the conduit to the pump. The figure also shows the measurement arrangement. Note in this regard that the reactor can be used for both etching and deposition.

The determination of intrinsic kinetics based on the experimental reactor in Fig. 10-13 can proceed as follows:

1. Establish a relationship between E_p/P and PL by varying pressure and electrode spacing for the desired excitation frequency and power input. In this process, the constant in Eq. (10.19) for efficient ignition of plasma can also be inferred. Also establish relationships between J_p and PL and those between V_p and PL. No substrates are involved in this phase of the experiment.
2. With the substrate placed on the powered electrode, run experiments in the ranges of substrate temperature and concentration of interest at constant ion energy levels.
3. Determine the intrinsic rate (kinetics) of etching or deposition with the aid of Eqs. (10.33) through (10.36) and Eqs. (10.41) through (10.44). Measure the main reactive neutral species concentration, J_p, and V_p.

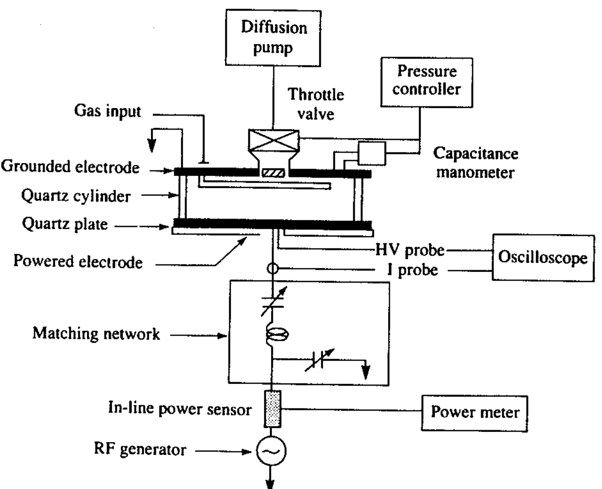

FIGURE 10-13
An experimental reactor for intrinsic kinetics.

4. Determine the homogeneous kinetics with the aid of Eqs. (10.45) through (10.47).

10.7 PLASMA REACTOR DESIGN AND ANALYSIS

There are no distinct configurational differences between plasma reactors for etching and those for deposition. The differences mainly lie in the operating conditions. This is not surprising since both take advantage of the surface modification by ions colliding with a substrate surface and of the generation of reactive neutral species in the plasma. In the case of deposition, the ion energy should be just sufficient to cause enhancement of the deposition rate; in etching, the same would be true except when anisotropy is critical, in which case a higher ion energy is required to obtain the desired directionality.

The main objectives in designing a plasma reactor are: uniformity in etching or deposition and minimum contamination by impurities at maximum possible throughput. In addition, achieving anisotropy is a major consideration in plasma etching. In both etching and deposition, but particularly in etching, there is a need to ensure that the substrate surface does not reach a high temperature, which causes temperature-related side effects. There are two main sources of contamination in plasma processing. The first is the undesired deposition of sputtered atoms on the substrate; the second is the undesired deposition

from the gas phase as in polymer formation and subsequent deposition. Although electrodes are usually coated with a material with a low sputtering rate and they are inert to reactive species, minimizing the contamination is still a major concern.

The size of a plasma reactor is determined by the number of wafers to be processed per batch, which determines the area of the reactor, and the diffusion characteristic length L, which in turn fixes the other dimensions. On the other hand, the performance of the reactor with respect to uniformity and anisotropy (in the case of etching) is determined by the operating conditions. The outermost constraint that has to be satisfied is the condition for efficient ignition given by Eq. (10.18) for a dc discharge and Eq. (10.19) for an rf (ac) discharge. The constraints are given in terms of PL for a dc discharge and P^2L for an rf discharge. In general, the highest maximum possible ion flux is desired for the maximum rate and is accomplished by increasing the pressure. However, the power required to ignite plasma becomes too excessive as the pressure is increased unless the diffusion length (or the electrode separation) is reduced. The chosen conditions should reflect these conflicting factors. It should be noted in this regard that, at high pressures, the electrode separation can be very small (of the order of 1 cm), and therefore the degree to which two electrodes are parallel to each other can have a significant effect on the uniformity because of the difference in electric field from one point to another.

The flow in plasma reactors, in most cases, is in the laminar flow regime. Depending on the pressure and the electrode separation, the flow can be in the transition to the molecular flow regime, in which case the usual viscous laws do not apply. According to Eqs. (6.4) and (6.6), the flow will be in transition to molecular flow at 0.01 torr for an electrode separation of a few centimeters. At the higher pressures (at most 10 torr) typical of plasma reactors and with small temperature differences, buoyancy (free convection) effects, if any, are negligible and the flow is stable.

A necessary condition for etching or deposition uniformity is that there should be negligible depletion of source gases. To be more direct, the concentration of the main reactive neutral species should be almost the same everywhere over the wafers being processed. This is not possible with the usual feeding arrangements, unless the number of wafers to be processed is quite small. If the source gas is distributed as in Fig. 10-7*a* (similarly as in the experimental reactor in Fig. 10-13), all wafers would be exposed to the same concentration, ignoring minor variations due to the flow pattern. For such a reactor, Eq. (10.45) applies, and it can be rewritten with the aid of Eq. (10.47) as follows:

$$v_p\left[k_G\left(\frac{HJ_p}{V_p}\right)C_m - k_r C_n^n\right] = QC_n + R_G A_s \tag{10.48}$$

where k_r is the recombination rate constant, and the order for the reaction, n, is usually one or two. Given the intrinsic kinetics and the desired rate of etching or deposition, the volumetric flow rate is then given by Eq. (10.48). An inherent restriction in writing Eq. (10.48) is that the source gas must not be depleted.

Otherwise, the relationship does not hold. Since the source gas is mainly depleted through the consumption of the reactive neutral species generated [Eq. (10.47)], one has

$$Q\,\Delta C_m = r_g = k_G\left(\frac{HJ_p}{V_p}\right)C_m \tag{10.49}$$

where ΔC_m is the concentration change due to the consumption. If one insists on almost constant C_m, say $\Delta C_m/C_m < \beta$, where β is a small number, one can write:

$$Q > \frac{k_G(HJ_p/V_p)}{\beta} \tag{10.50}$$

For less than 1 percent change, the value of β would be 0.01. Thus, Eq. (10.48) can be used with the restriction of Eq. (10.50).

Example 10.11. Reconsider the etching in Example 10.9. The following kinetics were reported by Stenger *et al.* (1987), which may be considered intrinsic:

$$R_G = 23.5\ (\text{cm/s})C_n \qquad \text{for } C_n = [\text{F}]$$

$$r_r = 0.57\ (\text{s}^{-1})C_n$$

Although it was reported that a maximum variation of 8 percent occurred at 100 sccm, 0.1 torr, and 25°C, assume for this example that true uniformity was attained under the conditions. The symmetric electrode area was 2450 cm^2, the plasma volume was 3850 cm^3, and the electrode spacing was 1.57 cm. Although the whole electrode area was not occupied by wafers, use the whole area in your calculation. Calculate the value of $k_G(J_p/V_p)$ for the etch rate of 0.15 μm/min. Also calculate the reactive fluorine atom concentration under the conditions.

Solution. From Eqs. (10.45) and (10.48) for the net rate of generation of reactive species, one has

$$r_G = k_G\left(\frac{HJ_p}{V_p}\right)\left(\frac{0.4P}{RT}\right) - 0.57C_n \tag{A}$$

where the ideal gas law has been used for C_m. Using Eq. (A) and R_G in Eq. (10.48) leads to

$$3850\left[\left(\frac{k_G J_p}{V_p}\right)\left(\frac{1.57 \times 0.4 \times 0.1}{760 \times 82 \times 298}\right) - 0.57C_n\right] = \left(\frac{760}{0.1}\right)\left(\frac{100}{0.60}\right)C_n + 2450R_G \tag{B}$$

From Example 10.9, $R_G = 2.764 \times 10^{-8}$ mol/(cm^2·s) and therefore $C_n = 1.176 \times 10^{-9}$ mol/cm^3. Substituting these values into Eq. (B) yields

$$\frac{k_G J_p}{V_p} = 5.49\ \text{cm}^{-1}$$

Note that the mass transport effect was negligible under the conditions.

It is instructive here to reexamine the role of V_p and J_p. It is well understood that a higher ion flux (J_p) but a relatively smaller ion energy (V_p or $V_p\lambda$) are

desirable. A higher ion flux enhances the rate and assures local uniformity (activated versus nonactivated surface), and the lower ion energy also enhances the rate [see Eq. (10.43)] but only up to the level where physical sputtering is minimal. It is therefore desirable to maximize the ratio J_p/V_p subject to the constraint that the ion energy is sufficient for the activation. This is also the desired direction for increasing the rate of generation of the reactive neutral species, as Eq. (10.47) shows. The equation is rewritten as follows:

$$r_g = k_G\left(\frac{HJ_p}{V_p}\right)\left(\frac{Py_i}{R_g T}\right) \tag{10.51}$$

where y_i is the feed mole fraction of the source species. Noting that J_p and V_p are determined by PL for given excitation power and frequency, the design essentially reduces to specifying P, L, Q, and power input for a given number of wafers to be processed since the specification of these parameters also determines the rate of generation of the reactive species.

The specifications of P, L, and the power input (or density) are to be considered now that Q is specified by the necessary condition for the uniformity. The specification can proceed in a systematic way when the intrinsic kinetics are available. One consequence of determining the kinetics in the form of Eq. (10.43) is that the "sufficient" ion flux is that corresponding to $AJ_p \gg 1$, or

$$J_p \gg \frac{1}{A} \tag{10.52}$$

Further, the intrinsic kinetics should also reveal the minimum required ion energy [$g(E_i)$ in Eq. (10.43)]. Therefore, one has the following condition for the ion energy E_i:

$$\beta_1 < E_i < \beta_2 \tag{10.53}$$

where E_i is either qV_p or that given by Eq. (10.40), that is, $\alpha_u E_p/P$ where α_u is a constant. Here, β_1 is the minimum sufficient ion energy for the desired surface modification or rate enhancement and β_2 is the maximum allowable ion energy above which physical sputtering becomes a problem. In general, one would keep the ion energy close to β_1. This is also in line with the desire to maximize HJ_p/V_p to obtain the maximum possible rate of generation of reactive neutral species. From Eq. (10.51) one has

$$\text{Maximize}\left(\frac{HPJ_p y_i}{V_p}\right) \tag{10.54}$$

Finally the condition of efficient plasma ignition for an rf discharge [Eq. (10.19)] at a given excitation frequency may be used:

$$P^2L = \text{constant} \tag{10.55}$$

The conditions of Eqs. (10.52) through (10.55) can be used along with the relationships for J_p and V_p, given in terms of PL, for the specification of the design and operating parameters. It is seen that the determination of intrinsic kinetics leads to the reactor specification.

Example 10.12. As discussed in Chap. 9, the ion energy has to be in excess of the threshold energy for physical sputtering to take place. For most metals, the threshold energy is approximately 20 eV, which means that physical sputtering would be minimal for the ion energy less than 15 eV (see Prob. 10.5). No one in the literature has yet provided all the information suitable for illustrating the above design procedures. Therefore, the data reported by Stenger *et al.* (1987) and Song (1988) will be adapted and combined for this example, although they studied two different plasma systems. Shown in Figs. 10-14 and 10-15 are the J_p and V_p adapted from the experimental data of Song. Specify Q, P, and L using the kinetic parameters of Stenger *et al.* and other information in Example 10.11. Assume a k_G value of 10^6 (cm·V/A), a value of 0.92 cm·torr² for the constant in Eq. (10.54), and β_1 and β_2 values of 10 and 15 eV. Also use 0.01 for β in Eq. (10.50).

The following relationships can be used:

$$\frac{E_p}{P} = \frac{1000}{PL} \tag{A}$$

$$\lambda_i\,(\text{cm}) = \frac{0.008}{P\,(\text{torr})} \tag{B}$$

Solution. As evident from Fig. 10-14, J_p increases with PL and then reaches a plateau at PL of 0.6. Thus, an equivalent of Eq. (10.52) is

$$PL > 0.6 \text{ cm·torr} \tag{C}$$

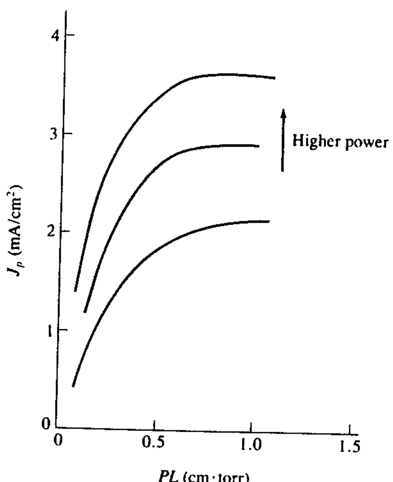

FIGURE 10-14
J_p versus PL.

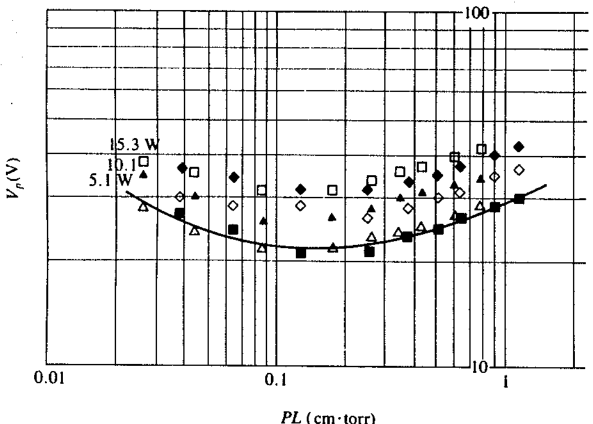

FIGURE 10-15
V_p versus PL.

According to the problem statement, $10 < E_i < 15$ eV. From Eqs. (B) and (10.40), $\alpha_u = 0.008q$ (cm·torr). Therefore,

$$10 < \frac{0.008E_p}{P} < 15 \qquad \text{(D)}$$

Using Eq. (A) in Eq. (D), one has

$$10 < \frac{8}{PL\ (\text{cm·torr})} < 15 \text{ eV}$$

This, when solved for PL, yields

$$0.53 < PL < 0.8 \text{ cm·torr} \qquad \text{(E)}$$

Equations (C) and (E) yield

$$0.6 < PL < 0.8 \text{ cm·torr} \qquad \text{(F)}$$

since Eq. (C) satisfies the lower limit in Eq. (E). The conditions imposed by Eq. (F) are shown shaded in Fig. 10-16. Since y_i is specified (0.4) in Example 10.11, Eq. (10.54) becomes

$$\text{Maximize}\left(\frac{HPJ_p}{V_p}\right) \qquad \text{(G)}$$

It is useful to note that L is essentially H/π since the radius is much larger than 2.405 cm [refer to Eq. (10.15)]. Therefore, Eq. (G) can be rewritten as

$$\text{Maximize}\left(\frac{PLJ_p}{V_p}\right) = \text{Maximize } I \qquad \text{(H)}$$

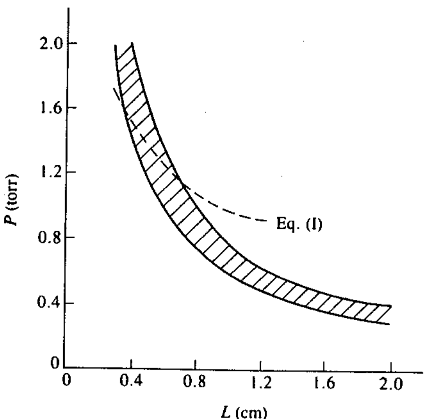

FIGURE 10-16
Permissible P and L.

Since J_p is already at its maximum possible, one is left with the maximum of PL/V_p. In the range given by Eq. (F), Fig. 10-15 reveals that V_p increases from approximately 24 to 28 volts when PL increases from 0.6 to 0.8 cm·torr. Now, one has, for Eq. (10.55),

$$P^2L = 0.92 \text{ cm·torr}^2 \qquad \text{(I)}$$

Equation (I) is shown in Fig. 10-16 as the dashed line. Since the maximum of I in Eq. (H) is that corresponding to $PL = 0.8$, the intersection between the line of PL of 0.8 and the dashed line gives the desired operating conditions, which correspond to P of 1.16 torr and L of 0.72 cm. To be reasonably within the boundaries specified by Eq. (F), one may choose a P of 1.1 torr and an L of 0.70 cm. Thus, the specifications are:

Pressure = 1.1 torr
Electrode spacing = 0.7 × 3.14 = 2.2 cm

Now that the specifications are available, the flow rate required for uniformity, with a gas distribution arrangement designed for uniform source concentration, can be obtained from Eq. (10.48):

$$3850\left[10^6\left(\frac{2.2 \times 2.0 \times 10^{-3}}{27}\right)\left(\frac{0.4 \times 1.1}{760 \times 82 \times 298}\right) - 0.57C_n\right]$$
$$= QC_n + 2450 \times 23.5C_n \qquad \text{(J)}$$

or

$$\frac{1.48 \times 10^{-2}}{C_n} = Q + 59{,}770 \qquad \text{(K)}$$

where it has been assumed that the mass transfer effect is negligible, which can be checked once the desired rate is selected. Note here that $J_p = 2$ mA/cm² and $V_p =$ 27 volts from the chosen conditions and Figs. 10-14 and 10-15. A plot of Q versus R_G ($=23.5C_n$) is given in Fig. 10-17. The vertical dotted line represents the restriction imposed by Eq. (10.50). As indicated by the solid line, specification of C_n

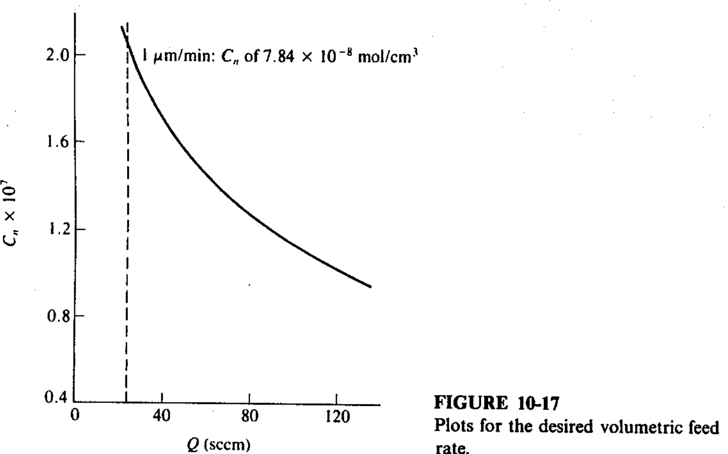

FIGURE 10-17
Plots for the desired volumetric feed rate.

(or R_G) fixes the flow rate, or vice versa. Suppose that an etch rate of 1.27 μm/min (or C_n of 10^{-7} mol/cm³) is desired. Then the corresponding flow rate should be 127 sccm. As examined in Example 10.9, the etching is not mass transfer limited. Thus, no further calculations are required. Note that the maximum rate is that corresponding to the flow rate of 24 sccm (Fig. 10-17).

This example illustrates the essence of the procedures one can follow in designing a plasma reactor, although details may vary depending on the system of interest. The design involves satisfying a number of conditions while maximizing the rate. It is made clear here that there are no essential differences between the design of plasma reactors for etching and those for deposition unless the former requires anisotropic etching.

The same procedures can be followed for asymmetrical systems, the only differences being the ion flux and ion energy. In etching, where anisotropy is critical, asymmetrical electrodes are used. The substrates are placed on the powered electrode, which is smaller than the grounded electrode. In this manner the voltage drop across the powered sheath is higher than the plasma potential drop, the ion flux is increased by the factor of A_g/A_p for the substrate on the powered electrode, and contamination can be minimized due to the smaller area exposed relative to a symmetrical system. As discussed in Example 10.7, the current flux ratio can be written as

$$\frac{J_{sp}}{J_p} = \frac{A_g}{A_p} \tag{10.56}$$

where A_g is the grounded electrode area and A_p is the powered electrode area. Although the ratio of potentials has been reported to vary with the fourth power of the area ratio (Koenig and Maissel, 1970), it can be shown (Zarowin, 1983; see

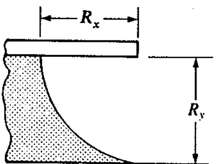

FIGURE 10-18
Definition of etch directionality.

Prob. 10.9) that the following holds for capacitive plasma:

$$\frac{V_p}{V_{sp}} = \begin{cases} A_p/A_g & L < \lambda \\ \left(\frac{A_p}{A_g}\right)\left(\frac{d_{sp}}{d_p}\right) & \text{otherwise} \end{cases} \tag{10.57}$$

where d_{sp} is the sheath thickness at the powered electrode and d_p is the sheath thickness at the grounded electrode. These values can be calculated using electrical measurements (Prob. 10.9). The same procedures used for symmetrical electrode design can be followed for the asymmetrical reactor design with the aid of Eqs. (10.56) and (10.57) for the additional parameter, A_g/A_p.

An additional factor that must be considered for directional etching is the desired degree of anisotropy. Referring to Fig. 10-18, the etch directionality, U, can be defined as

$$U = \frac{R_x}{R_y}$$

Complete anisotropy results when $U = 0$; complete isotropy occurs when $U = 1$. According to Zarowin (1983), the etch directionality is inversely proportional to the following:

$$\frac{1}{U} \propto \left(\frac{E_{sp}}{P}\right)\left(\frac{1 + M_i/M_n}{Q_i}\right) \tag{10.58}$$

where M_i is the ion mass, M_n is the mass of dominant neutral species and E_{sp} is the electric field across the sheath of the powered electrode where the substrate is placed. For a given plasma, the desired anisotropy can be attained if

$$\frac{E_{sp}}{P} > \text{constant} \tag{10.59}$$

An equivalent way of expressing this condition is to use P_w/P in place of E_{sp}/P for a given system where P_w is the applied rf power. The constant in this case, reported by Zarowin, is 1.4 W/torr for polysilicon etching by Cl_2-He plasma. As indicated by Eq. (10.58), the constant in Eq. (10.59) becomes larger when the dominant neutral species has a higher molecular weight. Thus, one would expect the constant to increase with decreasing content of helium in Cl_2-He plasma, as the experimental results of Zarowin show. Note that an equivalent form of Eq. (10.59) can be written as $J/P >$ constant. This means that a higher current flux results in a higher anisotropy.

For design purposes, the anisotropy requirement places the uppermost constraint on the range of PL allowed since E_{sp}/P can be correlated to PL, as shown in Fig. 10-12. The electrode area ratio gives an additional degree of freedom to work with the added constraint. The design procedures remain essentially the same as those for symmetric electrodes.

Analysis of a plasma reactor involves the same considerations as its design. However, the reactor transport of reactive and source species has to be considered in the analysis when the mode of gas distribution does not guarantee equal exposure of the wafers to the same concentrations of the species. This is typically the case with reactors being used in practice, such as the barrel, planar, and hexode reactors in Fig. 10-6. The transport of species in a planar plasma reactor (Stenger *et al.*, 1987) will be considered first. Mass balances for the reactive neutral species and the source species are

$$v_r \frac{\partial C_n}{\partial r} = D\left[\frac{1}{r}\frac{\partial}{\partial r}\left(r\frac{\partial C_n}{\partial r}\right) + \frac{1}{r^2}\frac{\partial^2 C_n}{\partial \theta^2} + \frac{\partial^2 C_n}{\partial z^2}\right] + k_g n_e C_m - r_r \qquad (10.60)$$

$$v_r \frac{\partial C_m}{\partial r} = D\left[\frac{1}{r}\frac{\partial}{\partial r}\left(r\frac{\partial C_m}{\partial r}\right) + \frac{1}{r^2}\frac{\partial^2 C_m}{\partial \theta^2} + \frac{\partial^2 C_m}{\partial z^2}\right] - mk_g n_e C_m \qquad (10.61)$$

where radial flow parallel to the electrodes has been assumed and m is a stoichiometric coefficient. The configuration and coordinates are shown in Fig. 10-19*a*. If the concentration is averaged over the electrode spacing and the wafers are

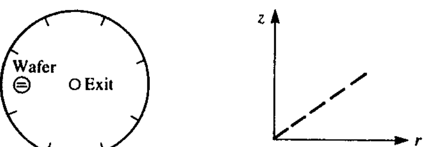

(*a*) Planar reactor

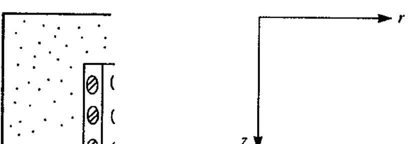

(*b*) Hexode reactor

FIGURE 10-19
Coordinate and geometry for two reactors.

placed symmetrically, the mass balances (see Prob. 10.16) reduce to

$$\frac{v_o r_o}{r}\frac{d\bar{C}_n}{dr} = \frac{D}{r}\frac{d}{dr}\left(r\frac{d\bar{C}_n}{dr}\right) - \frac{A_s r_c}{H} + k_g n_e \bar{C}_m - R_r \qquad (10.62)$$

$$\frac{v_o r_o}{r}\frac{d\bar{C}_m}{dr} = \frac{D}{r}\frac{d}{dr}\left(r\frac{d\bar{C}_m}{dr}\right) - mk_g n_e \bar{C}_m \qquad (10.63)$$

where v_o is the average bulk velocity at the outside radius r_o of the reactor boundary and R_r is the rate of recombination written in terms of $\bar{C}_n$. For the system considered in Example 10.9, C_n is the concentration of F atoms, C_m is the concentration of NF_3, $r_c = kC_n$, and $r_r = k_r C_n$. As shown in Prob. 10.16, the concentration difference between any normalized radial position x and the outlet $(x = 0)$ is proportional to the following:

$$\Delta\bar{C}_m \propto x^{\mu} I_{\mu}(\alpha x) \qquad (10.64)$$

where

$$\mu = \frac{v_o r_o}{2D} = \frac{\text{Pe}}{2}$$

$$\alpha = \left(\frac{mk_g n_e r_o^2}{D}\right)^{1/2}$$

and Pe is a Peclet number and I_{μ} is the modified Bessel function of order μ. One conclusion from Eq. (10.64) is that the concentration of the source species cannot be uniform unless the Peclet number approaches infinity, in which case the feed velocity approaches infinity. In such a case, the reactive neutral species are swept away by the flow and the rate of etching or deposition can become unacceptably low. An optimization for the uniformity leads only to a small window of acceptable operating conditions, and this is the reason why feeding arrangements that lead to uniform concentration over the wafers are being sought in practice. Note that the reactor transport, such as that represented by Eqs. (10.60) and (10.61), need not be considered if a feeding arrangement provides a uniform concentration over the wafers of interest.

The barrel reactor in Fig. 10-6 has a feeding arrangement similar to that for an LPCVD reactor. Here again, however, the trend is toward a feeding arrangement for uniform exposure of wafers to the same source species concentration. In such a case, the reactive species concentration at the edges of the wafers is the same for all wafers. This system was analyzed by Alkire and Economou (1985) in detail for the limiting case of no recombination. Under that restriction, the uniformity is guaranteed if the following condition is satisfied:

$$\frac{RG\rho_s}{1.5B_r C_o D M_w} < \tanh\left(\frac{1.203s}{R}\right) < 1 \qquad (10.65)$$

which is Eq. (6.49*a*) derived earlier for an LPCVD reactor. Here R is the wafer radius, G is the desired etch or deposition rate in length per time, ρ_s is the density of the material being etched or deposited, M_w is its molecular weight, C_o is the

concentration of the reactive neutral species at the wafer edges, B_r is the degree to which the uniformity is desired (0.01 for 1 percent deviation, for example), and s is the interwafer distance. When the reactor has a feeding arrangement similar to that for an LPCVD reactor (Fig. 10-6*b*), mass balance equations have to be solved first for the annular region between the wall and the metal grid for the plasma confined in the annulus, and then between the metal grid and the wafer edges for the reactive neutral species. The concentration of the reactive neutral species at the wafer edges can then be used for the transport between two adjacent wafers.

The hexode plasma reactor is essentially the same as the barrel CVD reactor. The only difference in the physical layout is that the inner hexode with side walls (on which the wafers are placed) is not inclined in the case of the plasma reactor to assure uniform electric field. If one treats the inner cylinder ideally with side walls as a perfect cylinder, the conservation equations, similar to Eqs. (10.60) and (10.61) for the hexode reactor, are

$$v_z \frac{\partial C_n}{\partial z} = D\left[\frac{1}{r}\frac{\partial}{\partial r}\left(r\frac{\partial C_n}{\partial r}\right) + \frac{\partial^2 C_n}{\partial z^2}\right] + k_g n_e C_m - r_r \tag{10.66}$$

$$v_z \frac{\partial C_m}{\partial z} = D\left[\frac{1}{r}\frac{\partial}{\partial r}\left(r\frac{\partial C_m}{\partial r}\right) + \frac{\partial^2 C_m}{\partial z^2}\right] - mk_g n_e C_m \tag{10.67}$$

where v_z is the velocity in the direction of flow and r is now the radial coordinate perpendicular to the flow direction (Fig. 10-19*b*). As discussed in Prob. 10.17, the equations, after averaging over the radial direction, reduce to

$$\frac{d\bar{C}_n}{dy} = \frac{1}{P_m}\frac{d^2\bar{C}_n}{dy^2} + t_f\left(k_g n_e \bar{C}_m - R_r - \frac{2R_i \bar{r}_c}{R_o^2 - R_i^2}\right) \tag{10.68}$$

$$\frac{d\bar{C}_m}{dy} = \frac{1}{P_m}\frac{d^2\bar{C}_m}{dy^2} - t_f(k_g n_e \bar{C}_m) \tag{10.69}$$

where the Peclet number P_m is given by Zv_z/D, $t_f = Z/v_z$, R_o and R_i are the radius for the outer and the inner cylinder, respectively, Z is the inner cylinder length, and y is the length coordinate normalized with respect to Z. The solutions to Eqs. (10.68) and (10.69) can be written for linear rate expressions as discussed in Prob. 10.17. As was the case in the planar plasma reactor, only a small window of operating conditions is available for near uniformity. A radial feeding arrangement along the inner reactor wall would be desirable. Another alternative is to introduce an inclined divider coaxially with the inner cylinder wall.

It should be clear from this section that the main design considerations are those for obtaining the plasma characteristics that are desired for the best possible performance of the plasma reactor. The design, therefore, involves satisfying a number of conditions for the desired plasma characteristics. The reactor transport effect is primarily determined by the way the source gas is distributed along the reactor. This effect can be eliminated by devising a feeding arrangement that leads to equal exposure of all wafers to the same source species concentration. Under such an arrangement, the gas-solid interface transport effect can still be present but can be compensated for to avoid a nonuniformity problem.

Finally, it should be kept in mind in using approximate relationships, in particular those related to plasma characteristics, that there are always exceptions to the relationships.

NOTATION

a, b, c	Width, depth, and length of a channel, respectively (L)
A	Constant in Eq. (10.41)
A_g, A_p	Area of ground and powered electrode, respectively (L^2)
A_s	Substrate area (L^2)
C	Concentration (mol/L^3)
C_b	Concentration of source species in bulk fluid; bulk concentration (mol/L^3)
C_d	Conductivity
C_m	Concentration of main neutral species (mol/L^3)
C_n	Concentration of reactive neutral species (mol/L^3)
C_p	Concentration of source species at a point near cold wall (mol/L^3)
C_s	Concentration of source species at substrate surface (mol/L^3)
d_a, d_i	Diameter of atom and ion, respectively (L)
D	Diffusivity; diffusivity of source species (L^2/t)
D_a	Ambipolar diffusivity (L^2/t)
E	Electric field (V/L); energy (E)
E_a	Activation energy (E)
E_i	Average ion energy (E)
E_o	Activation energy in absence of ions (E)
f	Frequency ($1/t$)
$f(C)$	Concentration dependence of rate
G	Linear growth rate (L/t)
H	Electrode spacing (L); cylinder length in Eq. (10.15) (L)
I_r	Root mean square current (I)
j	Ion flux (ion/L^2t)
J	Current density (current/L^2t)
k	Rate constant
k_B	Boltzmann constant
k_g	Rate constant for rate of generation of ions
k_m	Mass transfer coefficient (L/t)
k_o	Preexponential factor for rate constant
k_r	Rate constant for rate of recombination of reactive neutral species
L	Characteristic diffusion length (L)
m	Electron mass (M); constant exponent in Eq. (10.5); stoichiometric constant in Eq. (10.61)
M	Ion mass (M); molecular weight (M)
M_r	Reduced mass (M)

n Number density (number/L^3); constant exponent in Eq. (10.8)
n_a Atom number density (atom/L^3)
N_n Number density of neutral species (neutral molecule/L^3)
p_0 Permittivity of free space
P Pressure (P)
P_d Probability of no collision
P_i Collision probability
P_m Peclet number in Eq. (10.69)
P_{ia} Average of diffusion cross section in Eq. (10.4)
P_w Power (W)
Pe Peclet number defined in Eq. (10.64)
q Elementary charge (1.6×10^{-19} C)
Q Volumetric flow rate (L^3/t)
Q_c Collision cross section
Q_i Ionization collision cross section
r Radial coordinate (L)
r_c Intrinsic rate
r_G Net rate of generation
r_r Recombination rate
r_o Radius of a sphere in Eq. (10.15); radius of electrode on which substrates are placed
r_s Rate of sputtering (atoms/L^2t)
R_g Gas constant
R_G Observed rate
R_r Normalized r_r
S Sputtering yield (atoms/ion)
Sh Sherwood number defined in Eq. (10.35)
t_f Fluid residence time in a reactor (t)
t_r Average lifetime (t)
T Temperature (T)
U Etch directionality
v Velocity (L/t)
v_d Drift velocity (L/t)
v_f Average fluid velocity (L/t)
v_o Average bulk velocity at outside radius r_o in Eq. (10.62)
v_p Plasma volume (L^3)
v_r Radial velocity (L/t)
v_z Axial velocity (L/t)
V Potential (V)
V_a Applied voltage (V)
V_f Floating potential in Eq. (10.30) (V)
V_{dc} DC bias (V)
W Quantity defined by Eq. (10.37)
x r/H
y Mole fraction
z Axial coordinate (L)
Z Hexode reactor length (L)

Greek letters

α Quantity defined in Example 10.1; quantity defined in Eq. (10.64)
β Small number in Eq. (10.50)
β_1, β_2 Constant ion energies in Eq. (10.53)
λ Mean free path (L)
λ_t Townsend coefficient in Eq. (10.9)
λ_D Debye length (L)
μ Mobility; constant in Eq. (10.64)
ρ Density (M/L^3)
ω Angular frequency (radian/t)
ω_p Plasma frequency defined by Eq. (10.20) ($1/t$)

Subscripts

a Atom
e Electron
i Ion
g Ground electrode
m Main (source) neutral species
n Neutral species
p Plasma; ground electrode sheath
sp Powered electrode sheath

Superscript

— Average

Units

E Energy (ML^2/t^2)
L Length
M Mass
P Pressure (M/it^2)
t Time
T Temperature
V Volt

PROBLEMS

10.1. Show that Eq. (10.10) follows from Eqs. (10.1) and (10.9), assuming that D_eP is constant. The log-log plot in Fig. 10-8 is almost linear for N_2O for E/P less than 1 volt/(cm·torr). Determine the form of Eq. (10.10) in this range. Comment on the functional dependence of λ_t on E/P. The temperature may be combined into the

constant term. Calculate the electron mobility of N_2O plasma at 1 torr under an electric field of 1 volt/cm.

10.2. Consider a medium in which the density of electrons is the same as that of ions. Let this density be n and velocity be v_a, which are the same for both species. Since $j = j_i = j_e = v_a n$ and $n = n_i = n_e$, Eqs. (10-2) and (10.3) yield

$$j_i = -D_i \frac{dn}{dx} + \mu_i En \qquad \text{(A)}$$

$$j_e = -D_e \frac{dn}{dx} - \mu_e En \qquad \text{(B)}$$

Combining these to solve for En yields

$$En = \frac{D_i - D_e}{\mu_i - \mu_e} \frac{dn}{dx} \qquad \text{(C)}$$

Now $v_a n = j = -D_a(dn/dx)$, which defines the ambipolar diffusivity D_a. Using this definition, derive Eq. (10.11).

10.3. The characteristic diffusion length (fundamental mode) for hexode and barrel (with metal grid) plasma reactors with outer radius r_o and inner radius r_i can be expressed as

$$L^2 = \left[\left(\frac{B}{r_o}\right)^2 + \left(\frac{\pi}{H}\right)^2\right]^{-1}$$

where B is given in the following table:

r_o/r_i	1.2	1.5	2.0	2.5	3.0	3.5	4.0
B	15.701	6.270	3.123	2.073	1.549	1.234	1.024

For planar reactors, r_o is large and thus L is well approximated by H/π, where H is the electrode spacing. For hexode and barrel reactors, H, which is now the cylinder length, is large. Thus L is well approximated by r_o/B. Noting that H is of the order of 1 cm and r_o is of the order of at least one wafer radius, make conclusions on the relative magnitude of ion energies for the same operating pressure and excitation power density.

10.4. In some applications, plasma is generated outside a reactor and then fed to the reactor. For an average lifetime of ions of 10^{-3} s, calculate the residence time in the reactor for the exit ion concentration to be at least 10 percent of the inlet concentration. Calculate the time for both once-through (plug-flow) and well-mixed reactors.

10.5. Davis and Vanderslice (1963) give the following expression for ion energy (E_i) density distribution when the sheath thickness is large relative to the mean free path:

$$f(E_i) = (\lambda q E)^{-1} \exp\left(-\frac{E_i}{\lambda q E}\right)$$

where E is the electric field. The mean energy for this distribution is $\lambda q E$. Since the mean free path λ is inversely proportional to P, λE is proportional to E/P. Show that the distribution can be rewritten as follows:

$$f(E_i) = \left(\frac{\alpha_r q E}{P}\right)^{-1} \exp\left(-\frac{E_i P}{\alpha_r q E}\right) \qquad \text{where } \alpha_r = \lambda_r P_r$$

and the subscript r is for a reference case. For the same applied voltage, how would you expect the pressure to affect the ion energy distribution? Suppose for an electrode material the threshold energy is 20 eV. Determine the fraction of ions that have an energy level above the threshold energy for an electrode spacing of 1 cm at 1 torr.

10.6. In plasma processing, it is desirable to minimize sputtering so that the impurities due to sputtered atoms are minimized. For Prob. 10.5, calculate the applied voltage at which only 1 percent of the ions have an energy level higher than 20 eV. Do the calculations for 1 and 2 torr. Discuss your result.

10.7. For the hexode reactor, the length equivalent to H in Eq. (10.35) is that given by Eq. (6.32):

$$H_{eq} = R_o \ln\left(\frac{R_o}{R_i}\right)$$

For a hexode reactor with an outside radius of 25 cm (R_o) and R_o/R_i of 1.08, determine the concentration of F atoms at the substrate surface for etching as per Example 10.9. Determine the total pressure at which the ratio of surface to bulk concentration becomes larger than 0.99.

10.8. According to the experimental results of Coburn and Winters (1979), the rate of silicon etching is 0.5 nm/min when only XeF_2 gas is used. When an argon beam is introduced, the rate increases to 5 nm/min under identical conditions. Assuming surface temperature to be 600 K, calculate the change in the activation energy due to the ion bombardment.

10.9. For capacitive plasmas (excitation frequency higher than, say, 3 MHz), Zarowin (1983) gives the following relationship:

$$\frac{E_p}{E_{sp}} = \frac{A_p}{A_g} \qquad \text{(A)}$$

where E_p is the electrode field across the sheath of the grounded electrode, E_{sp} is the electrode field across the sheath of the powered electrode, A_p is the area of the powered electrode, and A_g is that of the grounded electrode. The average energy ions acquire in arriving at an electrode is equal to the force (qE_j, $j = p$ or sp) multiplied by the distance they travel. Thus, the ion energy E_i, when there are negligible collisions in the sheath, is given by

$$(E_i)_j = qE_j d_j \qquad \text{for } j = p \text{ or } sp \qquad \text{(B)}$$

where d is the sheath thickness. It follows from Eq. (B) that

$$(E_i)_j = qV_j \qquad \text{(C)}$$

When the pressure is relatively high, such that the sheath thickness is large relative to the mean free path, the distance ions travel is λ instead of d. Thus, the ion energy

$$(E_i)_j = qE_j\lambda = \frac{qV_j\lambda}{d_j} \tag{D}$$

Show that the following relationships (Song, 1988) hold:

$$\frac{(E_i)_p}{(E_i)_{sp}} = \begin{cases} \dfrac{V_p}{V_{sp}} = \left(\dfrac{A_p}{A_g}\right)\left(\dfrac{d_p}{d_{sp}}\right) & \text{when Eq. (C) holds} \quad \text{(E)} \\ \left(\dfrac{V_p}{V_{sp}}\right)\left(\dfrac{d_{sp}}{d_p}\right) = \dfrac{A_p}{A_g} & \text{when Eq. (D) holds} \quad \text{(F)} \end{cases}$$

According to Song, the ion flux at the powered electrode j_i is given by

$$j_i = \frac{I_r}{2\pi A_p[1 - (1/\pi)\cos^{-1}(-V_{dc}/V_a)]q} \tag{G}$$

10.10. For an asymmetric system in which the rms current is 100 mA at the powered electrode, determine the sheath potentials and current fluxes at both electrodes. Also obtain the sheath thicknesses at both electrodes. Use the following information:

$$-V_{dc} = 10 \text{ volts} \qquad V_a = 20 \text{ volts}$$

$$A_p = 10 \text{ cm}^2 \qquad A_g = 40 \text{ cm}^2$$

$$\text{Excitation frequency} = 13.56 \text{ MHz}$$

Assume that the pressure is high enough for the sheath thickness to be large relative to the ion mean free path.

10.11. For Prob. 10.10, calculate the ion energies at both electrodes and the ion flux at the powered electrode for the plasma at 1 torr and 300 K. Assume that ions and neutrals have the same mass and diameter and that the diameter is 0.5 nm, for which Eq. (10.39) reduces to

$$\lambda = (2^{1/2}\pi d^2 N)^{-1}$$

10.12. Show that a relationship between E_{sp}/P versus PL along with one between V_{sp} versus PL are sufficient, given the electrode areas, to obtain information on ion energy and ion flux for the design of a plasma reactor. List the equations necessary.

10.13. As the minimum dimension of devices decreases, it becomes increasingly more important to attain anisotropy at a lower ion energy so that the damage caused by ion bombardment does not lead to serious defect problems. Discuss whether an additional freedom can be gained by operating in the pressure region where the sheath thickness is smaller than the mean free path.

10.14. The rate of etching in a reactor decreases as the number of wafers placed increases. This effect is known as the loading effect (Mogab, 1977). The effect of volumetric flow rate on the etch rate is known to initially increase with increasing flow and then decrease, going through a maximum (Chapman and Minkiewicz, 1978). Although these effects have not been well documented for plasma deposition, the same effects are expected to occur in deposition as well. Although these effects cannot be described readily without solving reactor conservation equations for neutral and source species, they can be fully described for those reactors where the ... the same concentration for all wafers. For these reactors, Eqs. (10.48) and (10.49) apply:

$$v_p\left[k_G\left(\frac{HJ_p}{V_p}\right)C_m - k_r C_n\right] = QC_n + R_G A_s \tag{A}$$

$$Q[(C_m)_{in} - C_m] = k_G\left(\frac{HJ_p}{V_p}\right)C_m \tag{B}$$

where the order n in Eq. (10.48) has been assumed to be unity. Assuming that the mass transfer effect is negligible and that the rate of etching or deposition is first order with respect to the concentration of the reactive neutral species, that is, $R_G = kC_n$, find the flow rate at which the etching rate becomes the maximum. Also, illustrate the loading effect.

10.15. The concentration profile in the direction perpendicular to the flow can be approximated by a parabolic profile:

$$C = a_0 + a_1 y + a_2 y^2 \tag{A}$$

where the a_i values are constants to be determined and y is the distance from the substrate. Since $C = C_s$ at $y = 0$, Eq. (A) can be rewritten as

$$C = C_s + a_1 y + a_2 y^2$$

When there is no feed from the upper electrode (opposite the electrode on which wafers are placed) $D(dC/dy) = 0$ at $y = H$. Further, $C = C_p$ at $y = H$. Using these conditions in Eq. (A) yields

$$C = C_s + \frac{2(C_p - C_s)}{H}y - \frac{C_p - C_s}{H^2}y^2 \tag{B}$$

Based on Eq. (B) and Eqs. (10.33) and (10.34), derive the first part of Eq. (10.35). Discuss why the Sherwood number is unity when the source gas is fed through the upper electrode such that the concentration there is constant.

10.16. Show that Eqs. (10.60) and (10.61) reduce to Eqs. (10.62) and (10.63) when the concentrations averaged over the electrode spacing are used as follows:

$$\bar{C} = \frac{1}{H}\int_0^H C\,dz$$

For the solution of Eq. (10.63), write Eq. (10.63) as follows:

$$\frac{d^2\bar{C}_m}{dx^2} + \frac{1 - a_1}{x}\frac{d\bar{C}_m}{dx} - a_2\bar{C}_m = 0 \tag{A}$$

where

$$a_1 = \text{Pe} = 2\mu$$

$$a_2 = \frac{mk_g n_e r_o^2}{D} = \alpha^2$$

By substitution, show that the following is a solution:

$$\bar{C}_m = Bx^{\mu}I_{\mu}(\alpha x) \tag{B}$$

where D is an integration constant. For the boundary conditions of $\bar{C}_m = \bar{C}_i$ at $x = 1$ and $\bar{C}_m = \bar{C}_{out}$ at $r = 0$, show that the solution is

$$\frac{\bar{C}_m}{C_{in}} = \frac{C_{out}}{C_{in}} + \left(1 - \frac{C_{out}}{C_{in}}\right)\frac{x^{\mu} I_{\mu}(\alpha x)}{I_{\mu}(\alpha)} \tag{C}$$

Thus, the concentration change is proportional to $x^{\mu} I_{\mu}(\alpha x)$.

10.17. Define the average concentrations in Eqs. (10.68) and (10.69) by

$$\bar{C} = \frac{\int_{R_i}^{R_o} rC\,dr}{\int_{R_i}^{R_o} r\,dr}$$

Multiply both sides of the equations by r and integrate from R_i to R_o to obtain Eqs. (10.68) and (10.69) using the above definition. Use appropriate radial boundary conditions. For $r_r = k_r C_n$ and first-order deposition kinetics, obtain the solutions for $\bar{C}_n$ and $\bar{C}_m$. The boundary conditions are

$$\frac{d\bar{C}_i}{dy} = \frac{1}{P_m}[\bar{C}_i - (C_i)_f] \qquad \text{at } y = 0; \quad i = m \text{ or } n$$

$$\frac{d\bar{C}_i}{dy} = 0 \qquad \text{at } y = 1; \quad (C_i)_f = \text{feed concentration}$$

10.18. The electrical properties of an rf or dc plasma can be simulated by solving electron and ion conservation equations, Poisson's equation for the electric field, and the electron energy equation, if one assumes that the pressure is high enough for such a continuum model to be used (Thompson and Sawin, 1986). The electron and ion conservation equations are:

$$\frac{\partial n_e}{\partial t} = \nabla(\mu_e E n_e) + D_e \nabla^2 n_e + (k_+ - k_-)N n_e \tag{A}$$

$$\frac{\partial n_i}{\partial t} = \nabla(\mu_i E n_i) + D_i \nabla^2 n_i + (k_+ - k_-)N n_e \tag{B}$$

where n is the number density, μ is the mobility, D is the diffusivity, N is the number density of source gas, E is the electric field, k_+ and k_- are the ionization and attachment rate constants, respectively, and the subscripts i and e are for ions and electrons, respectively. Poisson's equation for this case is

$$\nabla^2 V = \frac{q(n_e - n_i)}{p_0} \tag{C}$$

The boundary conditions are

$$n_e = n_i = 0 \qquad \text{at electrodes}$$
$$V = 0 \qquad \text{at grounded electrode} \tag{D}$$
$$V = V_{dc} + V_a \sin(\omega t)$$

The first condition follows from the assumption that charged particles are neutralized at the electrodes. Suppose solutions are sought in the following forms (Thompson and Sawin, 1986):

$$n_e = k_e(t) g_e(x, t)$$
$$n_i = k_i(t) g_i(x, t) \tag{E}$$

Show that, based on Eqs. (A), (D), and (E) for n_e, under certain conditions g_e is almost time invariant.

REFERENCES

Alkire, R. C., and D. J. Economou: *J. Electrochem. Soc.*, vol. 132, p. 648, 1985.
Brown, S. C.: *Introduction to Electrical Discharges in Gases*, Wiley, New York, 1966.
Chapman, B. N.: *Glow Discharge Processes*, Wiley, New York, 1980.
——— and V. J. Minkiewicz: *J. Vac. Sci. Technol.*, vol. 15, p. 239, 1978.
Cho, A.: *Conference Proceedings, Compound Semiconductor Growth, Processing and Devices for the 1990s*, University of Florida, Gainesville, October 1987.
Coburn, J. W., and H. F. Winters: *J. Appl. Phys.*, vol. 50, p. 3189, 1979.
Dalvie, M., K. F. Jensen, and D. B. Graves: *Chem. Eng. Sci.*, vol. 41, p. 653, 1986.
Davis, W. D., and T. A. Vanderslice: *Phys. Rev.*, vol. 131, p. 219, 1963.
Edelson, D., and D. L. Flamm: *J. Appl. Phys.*, vol. 56, p. 1552, 1984.
Fraser, D. B.: in S. M. Sze (ed.), *VLSI Technology*, chap. 9, McGraw-Hill, New York, 1983.
Golan, V. E., *et al.*: in S. Brown (ed.), *Fundamentals of Plasma Physics*, Wiley, New York, 1979.
Heinecke, R. A.: *Solid State Elect.*, vol. 18, p. 1146, 1975.
Hirschfelder, J. O., C. F. Curtis, and R. B. Bird: *Molecular Theory of Gases and Liquids*, Wiley, New York, 1964.
Irving, S. M.: *Solid State Technol.*, vol. 14(6), p. 47, 1971.
Koenig, H. R., and L. I. Maissel: *IBM J. Res. Dev.*, vol. 14, p. 168, 1970.
Kumagai, H. Y.: in McD. Robinson *et al.* (eds.), *Chemical Vapor Deposition, 1984*, p. 198, The Electrochemical Society, Pennington, N.J., 1984.
Luscher, P. E., and D. M. Collins: in B. R. Pamplin (ed.), *Design Considerations for MBE Systems*, Pergamon, London, 1981.
McDaniel, E. W.: *Collision Phenomena in Ionized Gases*, Wiley, New York, 1964.
Maddox, R. L., and H. L. Parker: *Solid State Technol.*, p. 107, April 1978.
Maissel, L.: in L. Maissel and R. Glang (eds.), *Handbook of Thin Film Technology*, chap. 3, McGraw-Hill, New York, 1970.
Mathad, G. S.: *Solid State Technol.*, p. 221, April 1985.
Mogab, C. J.: *J. Electrochem. Soc.*, vol. 124, p. 1262, 1977.
Morgan, R. A.: *Plasma Etching in Semiconductor Fabrication*, Elsevier, Amsterdam, 1985.
Reinberg, A. R.: U.S. patent 3,757,733, 1975.
Rosler, R. S., and G. M. Engle: *Solid State Technol.*, p. 172, April 1981.
Saito, J., T. Igareski, T. Nakamura, K. Kondo, and A. Shibatoni: 4th International Conference on MBE, York, England, September 1986.
Song, M. K.: "Application of Impedance Analysis to Reactive Ion Etching of Silicon and Teflon," PhD Thesis, Drexel University, 1988.
Stenger, H. G., Jr., H. S. Caram, C. F. Sullivan, and W. M. Russo: *Ass. Ind. Chem. Engrs J.*, vol. 33, p. 1187, 1987.
Thompson, B. E., and H. H. Sawin: *J. Appl. Phys.*, vol. 60, p. 89, 1986.
Tokauaga, C., and D. W. Hess: *J. Electrochem. Soc.*, vol. 127, p. 928, 1980.
Weiss, A. D.: *Semicond. Int.*, vol. 6, p. 88, 1983.
Zarowin, C. B.: *J. Electrochem. Soc.*, vol. 130, p. 1144, 1983.